

Atmospheric Radiative Transfer and Climate

3.1 PHOTONS AND MINORITY CONSTITUENTS

The energy that sustains warmth and life at the surface of Earth travels from the Sun in the form of radiation. The interaction of incoming solar radiation with the atmosphere and the surface determines the total amount of solar energy absorbed and the distribution of solar heating among atmospheric layers and the surface. Because the atmosphere is relatively transparent to solar radiation, about half of the incoming solar radiation is absorbed at the ocean or land surface (Fig. 2.4). To achieve energy balance, heat provided by the absorption of solar radiation must be returned to space by emission from Earth. Transmission of thermal infrared radiation through the atmosphere and the upward transport of heat by atmospheric motions are the critical factors in returning energy to space. The transmission properties of the atmosphere are determined by its gaseous composition and the nature of aerosols and water clouds present in it. The composition of the atmosphere is such that it efficiently absorbs and emits thermal infrared radiation. The efficient absorption and emission of thermal infrared radiation by the atmosphere, combined with its relative transparency to solar radiation, causes the surface to be much warmer than it would be in the absence of an atmosphere.

Molecules that comprise a tiny fraction of the atmosphere's mass do nearly all the absorption and emission by the air. The dependence of the climate on the abundance of these minority constituents makes the climate sensitive to natural and human-induced changes in atmospheric composition. Relatively small changes in composition can affect the flow of energy through the climate system and thereby produce surprisingly large climate changes.

To understand how climate depends on atmospheric composition, it is necessary to understand the nature of electromagnetic radiation and the physical processes through which it interacts with gases and particles.

The equation of radiative transfer forms the mathematical basis for keeping track of these physical processes in an aggregate sense, so that radiative energy fluxes and heating rates can be computed. One-dimensional models, in which the vertical fluxes of energy by radiation are calculated from the radiative transfer equation, can be used to estimate the effect of trace-gas concentrations, clouds, and aerosols on the global mean surface temperature.

3.2 THE NATURE OF ELECTROMAGNETIC RADIATION

Electromagnetic radiation can be thought of either as a wave or as a particle that represents the movement of energy through space. For scattering of light by particles and surfaces, electromagnetic wave theory is most helpful. When considering absorption and emission of radiation, it is useful to think of radiant energy as discrete parcels of energy that we call photons. The speed of electromagnetic radiation in a vacuum is a constant $c^* = 3 \times 10^8 \text{ ms}^{-1}$. This means that frequency ν and wavelength λ are inversely related in a one-to-one correspondence.

$$\nu = \frac{c^*}{\lambda}; \quad \lambda = \frac{c^*}{\nu} \quad (3.1)$$

High frequencies correspond to short wavelengths, whereas low frequencies correspond to long wavelengths. Most of the time we will describe radiation in terms of its wavelength, which we will give in millimeters ($\text{mm} = 10^{-3} \text{ m}$), micrometers ($\mu\text{m} = 10^{-6} \text{ m}$), or nanometers ($\text{nm} = 10^{-9} \text{ m}$). In explaining the photoelectric effect, Einstein postulated that radiant energy exists and propagates in quantum bits called photons. If we think of light as photons, then a photon has an energy, E_ν , that is proportional to its frequency.

$$E_\nu = h\nu \quad (3.2)$$

where $h = 6.625 \times 10^{-34} \text{ Js}$ is Planck's constant. Therefore, high-frequency, short-wavelength radiation has more energy per photon than low-frequency radiation.

Most of the Sun's radiant energy output is contained between wavelengths of 100 nm and 4 μm , and consists of ultraviolet, visible, and near infrared radiation. Of the Sun's emission, 99% comes from the sum of the visible (0.4–0.75 μm) and near infrared (0.75–5 μm) portions of the spectrum. Ultraviolet radiation makes up less than 1% of the total, but is nonetheless important because of its influence in the upper atmosphere,

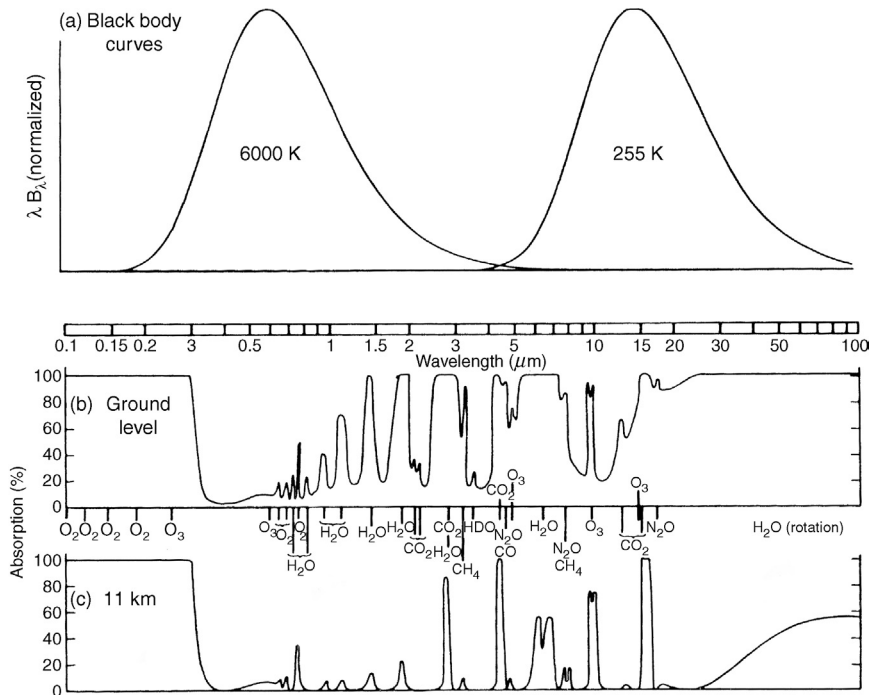


FIGURE 3.1 The normalized blackbody emission spectra for the Sun (6000 K) and Earth (255 K) as a function of wavelength (a). The fraction of radiation absorbed while passing from the surface to the top of the atmosphere as a function of wavelength (b). The fraction of radiation absorbed from the tropopause to the top of the atmosphere as a function of wavelength (c). The atmospheric molecules contributing the important absorption features at each frequency are indicated. *From Goody and Yung (1989). Reprinted with permission from Oxford University Press.*

and because it is harmful to life if it reaches the surface. Earth's energy emission is almost all contained between about 4 μm and 200 μm , and is therefore entirely thermal infrared (Fig. 3.1).

3.3 DESCRIPTION OF RADIATIVE ENERGY

The energy of radiation is measured by its intensity or radiance. The monochromatic intensity describes the amount of radiant energy (dF_v) within a frequency interval (v to $v + dv$) that will flow through a given increment of area (dA) within a solid angle ($d\omega$) of a particular direction in a time interval (dt).

$$dF_v = I_v \cos \theta d\omega dA dv dt \quad (3.3)$$

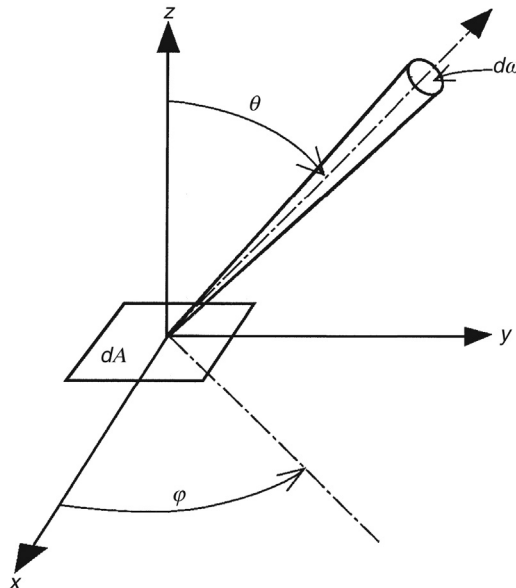


FIGURE 3.2 The angles that define the radiance flowing through a unit area dA in the x - y plane. These angles are in the direction defined by the zenith angle θ , and the azimuth angle φ , and within the increment of solid angle $d\omega$.

The direction is defined by the zenith angle, θ , and the azimuth angle, φ , as shown in Fig. 3.2. The magnitude of the radiant intensity, I_v , is given in energy per unit time, per unit area, per unit of frequency interval, per unit of solid angle, or watts per meter squared per hertz per steradian. In this book, we will be concerned mostly with the total energy per unit frequency passing across a unit area of a plane surface from one side to the other. To obtain this quantity, we integrate the radiant intensity over all solid angles in a hemisphere. To do this we need to make use of the definition of an increment of solid angle, which is equivalent to the area on the surface of a sphere with unit radius.

$$d\omega = \sin \theta d\theta d\varphi \quad (3.4)$$

Inserting (3.4) into (3.3) and integrating over the upper hemisphere we obtain

$$F_v = \int_0^{2\pi} \int_0^{\pi/2} I_v(\theta, \psi) \cos \theta \sin \theta d\theta d\varphi \quad (3.5)$$

This quantity is called the *spectral irradiance*. If F_v is integrated over all frequencies, we obtain the *irradiance*, which has units of watts per meter squared.

$$F = \int_0^{\infty} F_v dv \quad (3.6)$$

When a beam of radiation encounters an object such as a molecule, an aerosol particle, or a solid surface, several possible interactions between the radiation and the object can take place. The radiation can pass the object unchanged, which is called *perfect transmission*. The radiation can change direction without a change in energy, which is *pure scattering*. The radiation can be *absorbed*, where it ceases to exist and its energy is transferred to the object. The probability that a photon will be scattered, absorbed, or transmitted depends on the frequency of the radiation and the physical properties of the object it encounters. Pure water droplets in clouds scatter visible radiation very effectively with relatively little absorption. Water vapor and carbon dioxide are very effective absorbers of thermal infrared radiation at certain frequencies. Matter can also add to the intensity of a beam of radiation by emitting radiation in the direction of the beam. Emission of radiation by matter depends on the substance's physical properties and temperature.

3.4 PLANCK'S LAW OF BLACKBODY EMISSION

The intensity of radiation in a cavity in thermodynamic equilibrium is given uniquely as a function of frequency and temperature by Planck's law. An object that absorbs all radiations incident on it is called a *blackbody*. A blackbody with temperature T emits radiation at frequency ν with an intensity given by Planck's law:

$$B_\nu(T) = \frac{2h\nu^3}{c^{*2}} \frac{1}{(e^{h\nu/kT} - 1)} \quad (3.7)$$

where $h = 6.625 \times 10^{-34}$ Js (Planck's constant), $k = 1.37 \times 10^{-23}$ JK⁻¹ (Boltzmann's constant), $c^* = 3 \times 10^8$ ms⁻¹ (speed of light), ν is the frequency of radiation in s⁻¹, T is the temperature in Kelvins.

The Stefan–Boltzmann law is an integral of Planck's law over all frequencies and over all angles in a hemisphere, and expresses the strong dependence of energy emission on temperature.

$$\pi \int_0^\infty B_\nu(T) d\nu = \sigma T^4 \quad (3.8)$$

The factor of π arises from the integration over one hemisphere, assuming that the emission is independent of angle (isotropic). The Stefan–Boltzmann constant defined in (2.5) can be expressed in terms of the more fundamental constants of Planck's law:

$$\sigma = \frac{2\pi^5 k^4}{15 c^{*2} h^3} \quad (3.9)$$

Planck's law of blackbody radiation contains within it Wien's law of displacement, which states that the wavelength of maximum emission is inversely proportional to temperature. That is, the hotter the object, the higher the frequency and the shorter the wavelength of emitted radiation. Note that for terrestrial temperatures (~ 255 K) the emission peaks around $10\text{ }\mu\text{m}$, whereas for the temperature of the Sun's photosphere (~ 6000 K) the emission peaks around $0.6\text{ }\mu\text{m}$ (Fig. 3.1). The energy emission from both the Sun and Earth become very small near $4\text{ }\mu\text{m}$, so that the frequencies at which they emit are almost completely distinct for energetic purposes. We can thus speak of solar and terrestrial radiation as separate entities. In climatology, solar radiation is often called *shortwave* radiation and terrestrial radiation is called *longwave*.

3.5 SELECTIVE ABSORPTION AND EMISSION BY ATMOSPHERIC GASES

In considering the global energy balance of Earth, we found that the effective emission temperature is 255 K, which is much less than the observed global mean surface temperature of 288 K. The explanation for this disparity is found in the different transmission properties of the atmosphere for terrestrial and solar radiation. The atmosphere is relatively transparent to solar radiation, whereas it is nearly opaque to terrestrial radiation. To understand the fundamental reasons behind this “greenhouse effect,” we must understand a little about the interaction of radiation with matter.

In deriving his law of blackbody radiation, Planck found it necessary to postulate that the energy levels of an atomic or molecular oscillator are limited to a discrete set of values that satisfy

$$E_v = nhv \quad (n = 0, 1, 2, \dots) \quad (3.10)$$

Equation (3.10) describes a set of discrete energy levels that differ one from the next by an amount $h\nu$. The oscillator may represent the periodic motions of an atom or molecule. A transition from one energy level to another, called a quantum jump, corresponds to the release or capture of an amount of energy equal to $h\nu$. One way to accomplish this energy transition is for the molecule to emit or absorb a photon of energy $h\nu$. This quantization effect only becomes apparent for very small oscillators such as molecules or atoms. For macroscopic oscillators such as a pendulum or a spring and weight apparatus, the amount of energy represented by $h\nu$ is too small to be noticed in comparison to the total energy of the system.

A photon is emitted from a substance in some finite amount of time ($\leq 10^{-8}$ s) then travels through space until it is absorbed. If it approaches a mass such as an air molecule or a solid particle, the photon can change

phase or direction, a process called *scattering*, or it can be absorbed. When a photon is absorbed, it ceases to exist and its energy is transferred to the substance that absorbed it. The energy of a molecule can be stored in vibrational, rotational, electronic, or translational forms.

$$E_{\text{Total}} = E_{\text{Translational}} + E_{\text{Rotational}} + E_{\text{Vibrational}} + E_{\text{Electronic}} \quad (3.11)$$

A molecule in the atmosphere can absorb a photon only if the energy of the photon corresponds to the difference between the energy of two allowable states of the molecule. Each mode of energy storage in a molecule corresponds to a range of energies, with electronic transitions corresponding to the largest energy differences and rotational transitions corresponding to the smallest. Allowable transitions between energy levels of the molecules making up the atmosphere determine the frequencies of radiation that will be efficiently absorbed and emitted by the atmosphere. If no transitions correspond to the energy of a photon, then it will have a good chance to pass through the gaseous atmosphere without absorption.

3.5.1 Translational or Kinetic Energy (Temperature)

Translational energy corresponds to the gross movement of molecules or atoms through space and is not quantized. At terrestrial temperatures, the kinetic energy of a molecule is generally small as compared to the energy required for vibrational transition. Collisions between molecules can carry away or supply energy during interactions between photons and matter, and this plays an important role in broadening the range of frequencies of radiation that can be absorbed by a particular transition between molecular energy levels. The Doppler effect associated with the movement of molecules can also broaden the range of frequencies absorbed or emitted by a particular energy transition of the molecule.

3.5.2 Rotational Energy

A macroscopic object such as a child's top can store an amount of energy that, in effect, varies continuously with its rotation rate. For tiny objects such as molecules in the atmosphere, the energy of rotation is quantized and can take on only discrete values. *Rotational energy transitions* involve energy changes that correspond to the energy of photons with wavelengths shorter than about 1 cm.

3.5.3 Vibrational Energy

Atoms are bonded together into stable molecules when the forces of attraction and repulsion are in balance at the appropriate interatomic distance. Molecular energy can be stored in the vibrations about this stable point. The states of the molecule and the allowable energy levels are again

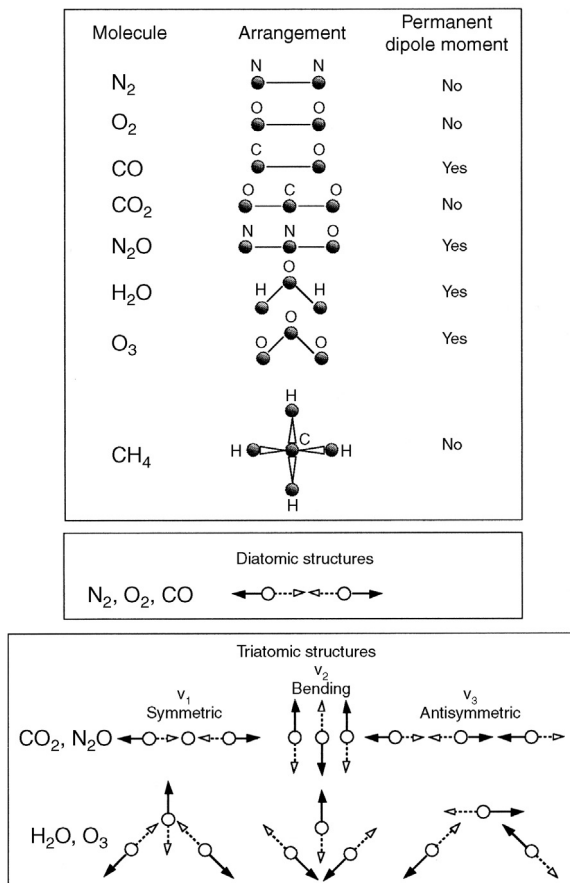


FIGURE 3.3 Schematic diagrams showing the vibrational modes of diatomic and triatomic molecules. From McCartney (1983). Reprinted with permission from Wiley and Sons, Inc.

quantized. Vibrational transitions require a photon with a wavelength of less than 20 μm . There are three independent modes of vibration for a triatomic molecule such as CO_2 : two stretching modes and one bending mode (Fig. 3.3).

A symmetric, linear molecule such as CO_2 has no permanent dipole moment, since it looks the same from both ends. For this reason, it has no pure rotational transitions. During vibrational transitions the CO_2 molecule develops temporary dipole moments so that rotational transitions can accompany a vibrational transition. The combination of possible vibrational and rotational transitions allows the molecule to absorb and emit photons at a large number of closely spaced frequencies, composing an absorption band.

Water vapor is a good absorber of terrestrial radiation because it is a bent triatomic molecule. Because it is bent, it has a permanent dipole moment and therefore has pure rotation bands in addition to vibration-rotation bands.

Vibration-rotation bands and pure rotation bands of polyatomic molecules account for the longwave absorption of the clear atmosphere that is shown in Fig. 3.1. The bending mode of CO₂ produces a very strong vibration-rotation absorption band near 15 μm, which is very important for climate and critical for the stratosphere where it accounts for much of the longwave absorption and emission. This absorption feature is particularly important because it occurs near the peak of the terrestrial emission spectrum. Water vapor has an important vibration-rotation band near 6.3 μm, and a densely spaced band of pure rotational lines of water vapor strongly absorbs terrestrial emission at wavelengths greater than about 12 μm. The rotational lines of water vapor are strong ones, and do not require a lot of water mass to be important. For this reason they dominate the cooling of the upper troposphere, where the specific humidity is fairly low. Between these two water-vapor features absorption by water vapor is relatively weak, and so this wavelength region is called the *water-vapor window*, since only in this frequency range can longwave radiation pass relatively freely through the atmosphere (see middle panel of Fig. 3.1 and Fig. 3.4). In the middle of this atmospheric window sits the 9.6-μm band of ozone. Together, all these absorption features make the troposphere nearly opaque to longwave radiation. Complicating this picture a little bit is the continuum absorption by water vapor. When the water vapor concentration is high, as in the warm tropics near the surface, radiation is weakly absorbed and emitted at all thermal wavelengths by water molecules that stick together (dimers). Thus in warm humid regions, continuum absorption by water-vapor molecules causes some more significant absorption in the window region between 8 μm and 12 μm.

Significant absorption of solar radiation by vibration-rotation bands of atmospheric gases occurs at near-infrared wavelengths between about 1 μm and 4 μm, mostly by water vapor and carbon dioxide (Figs. 3.1 and 3.4). These absorption features account for most of the absorption of solar radiation by air molecules in the troposphere. Visible wavelengths (~0.3–0.8 μm) are virtually free of gaseous absorption features, giving the cloud-free atmosphere its transparency in these wavelengths. Because a large fraction of the Sun's radiant energy is contained in visible wavelengths (Fig. 3.1), solar radiation penetrates relatively freely to the surface, where it provides heat and light.

3.5.4 Photodissociation

If a photon is sufficiently energetic, it can break the bond that holds together the atoms in a molecule. To photodissociate the molecules in the atmosphere, photons with energy corresponding to wavelengths shorter

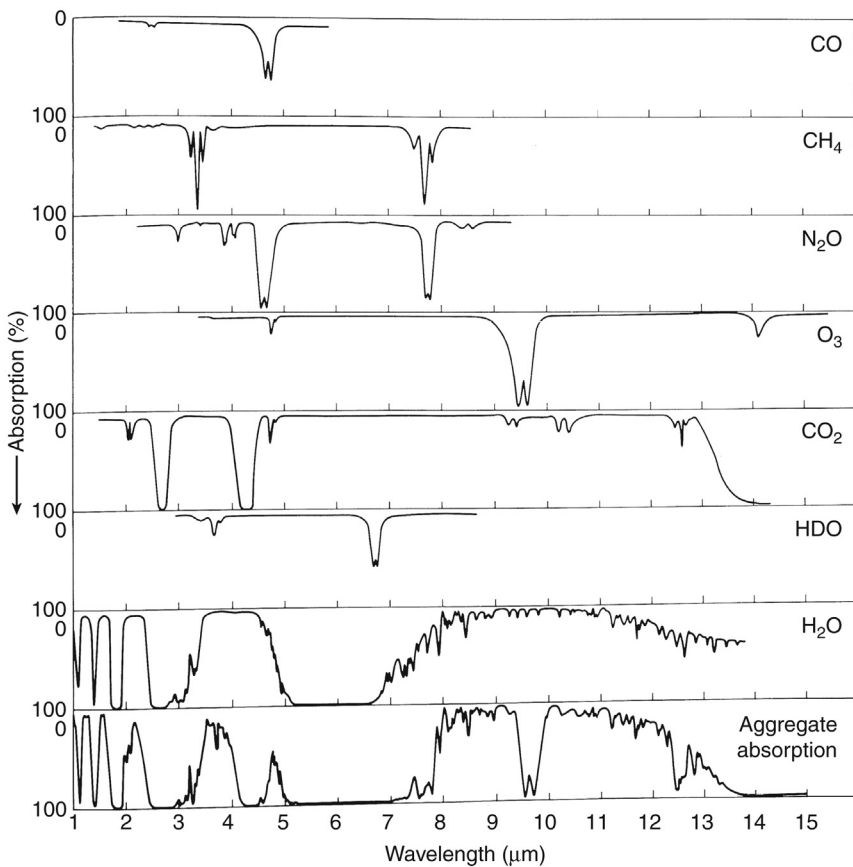


FIGURE 3.4 Infrared absorption spectra for various atmospheric gases. From Valley (1965). Used with permission from McGraw-Hill, Inc.

than $\sim 1 \mu\text{m}$ are required. Oxygen is dissociated in the upper atmosphere by radiation with wavelengths shorter than $\sim 200 \text{ nm}$. When a photon participates in the dissociation of a molecule, it ceases to exist and the atmosphere absorbs its energy.

Ozone is a bent molecule made up of three oxygen atoms and is more loosely bonded than molecular oxygen. It can be dissociated by radiation between 200 nm and 300 nm, and ozone absorbs most of the radiation in this band before it reaches the surface (Fig. 3.1), where it would otherwise do considerable damage to life.

3.5.5 Electronic Excitation

Photons with energies in excess of that corresponding to a wavelength of $1 \mu\text{m}$ can also excite the electrons in the outer shell of an atom.

Sometimes when oxygen or ozone is dissociated by solar radiation, one or both of the resulting oxygen atoms are in an electronically excited state.

3.5.6 Photoionization

If the wavelength of radiation is shorter than about 100 nm, then it can actually remove electrons from the outer shell surrounding the nucleus and produce ionized atoms. This process is responsible for the ionosphere. If the photon is even more energetic (shorter than ~ 10 nm), it can also photoionize the inner shell of electrons.

3.5.7 Absorption Lines and Line Broadening

The atmosphere is a very effective absorber at those discrete frequencies corresponding to an energy transition of an atmospheric gas. We may call each of these discrete absorption features an *absorption line*. The collection of such absorption lines in a particular frequency interval can be called an *absorption band*. Vibrational and rotational transitions are of primary interest for absorption and emission of terrestrial radiation in the atmosphere, since the energy levels associated with these transitions correspond to the energies of photons of thermal infrared radiation. Polyatomic molecules, such as H_2O , CO_2 , O_3 , CH_4 , N_2O , and many others, have vibration rotation bands of importance in the thermal infrared portion of the electromagnetic spectrum (Fig. 3.4, Table 3.1). Since lower energies are required for

TABLE 3.1 Wavelengths of Vibrational Modes of Some Important Atmospheric Molecules

Species	Vibrational modes		
	v1	v2	v3
CO	4.67		
CO_2		15.0	4.26
N_2O	7.78	17.0	4.49
H_2O	2.73	6.27	2.65
O_3	9.01	14.2	9.59
NO	5.25		
NO_2	7.66	13.25	6.17
CH_4	3.43	6.52	3.31
CH_4	5.25		

Units are in microns (μm).

From Herzberg and Herzberg © 1957 from McGraw Hill, Inc. and Shimanouchi, 1967a,b, 1968.

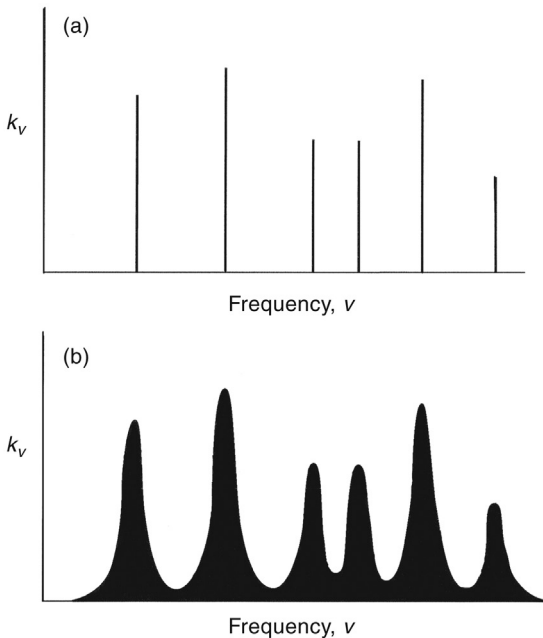


FIGURE 3.5 Hypothetical line spectrum (a) before broadening, (b) after broadening.

rotational transitions, molecules with pure rotational transitions can give a densely packed band of rotation lines. This is the case for water vapor, which has many rotational absorption lines at closely spaced frequencies, which form a rotation band that absorbs much of Earth's emission at wavelengths between $12 \mu\text{m}$ and $200 \mu\text{m}$. Many of these lines are very strong, in the sense that photons with these wavelengths are very likely to be absorbed by water, and they are very important in the cold upper troposphere where water vapor is present, but not very abundant.

A portion of a line absorption spectrum might look like Fig. 3.5a. Lines are not always evenly spaced or equally strong, since some transitions are more probable than others. The line width depends on broadening processes, which include natural, pressure, and Doppler broadening. After broadening, the absorption spectrum may have substantial absorption between the line centers (Fig. 3.5b).

Natural broadening is associated with the finite time of photon emission or absorption and with the uncertainty principle. If we know the energy exactly, then we can only know the frequency to a finite precision. This mechanism is usually less important than pressure or Doppler broadening.

Pressure broadening (also called *collision broadening*) is brought about by collisions between molecules or atoms, which can supply or remove small amounts of energy during radiative transitions, thereby allowing photons

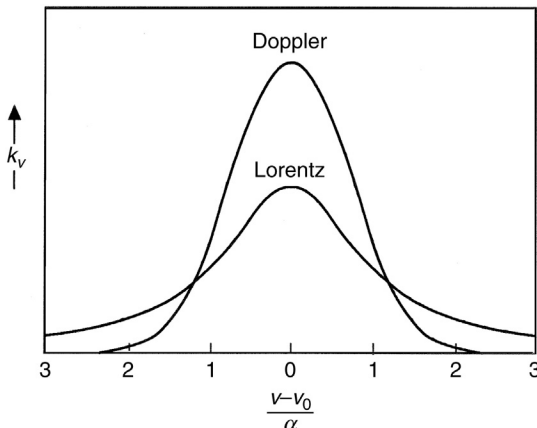


FIGURE 3.6 Line shapes produced by pressure (Lorentz line shape) and Doppler broadening for the same line width (α) and intensity at some central frequency v_0 . From Goody and Yung (1989). Reprinted with permission from Oxford University Press.

with a broader range of frequencies to produce a particular transition of a molecule. This is the primary broadening mechanism in the troposphere.

Doppler broadening results from the movement of molecules relative to a photon, which can cause the frequency of radiation to be Doppler-shifted. This again allows a broader range of frequencies of radiation to effect a particular molecular transition. Doppler broadening becomes the dominant mechanism at low pressures (high altitudes), where collisions are less frequent.

Pressure broadening is dominant in the troposphere and gives the lines a characteristic shape and width (Fig. 3.6). The line shape is important. Absorption is most probable at the frequency corresponding to the change in the energy of the molecule between two states, and this frequency locates the line center. The probability of absorption decreases away from the line center but remains significant at some frequency interval away from it. These weak absorption features away from the line center are called the *wings* of the absorption line. For strong absorption lines, the radiation at frequencies near the center of the line is completely absorbed after traveling a relatively small distance through the atmosphere. Under these conditions, most of the transmission of energy is carried by frequencies in the wings of the absorption lines, where absorption is weaker. Pressure broadening, which produces the Lorentz line shape and has broad wings, is particularly effective at producing absorption and emission far from the line centers.

Most of the atmosphere is made up of molecular nitrogen and oxygen. These are diatomic molecules, which have no dipole moment even when

vibrating. Therefore, they have no vibration–rotation transitions at the small energies corresponding to terrestrial radiation. Thus, it is the minor trace concentrations of polyatomic molecules that determine the infrared transmissivity of the atmosphere. The most important gases are water vapor, carbon dioxide, and ozone (in that order), but many other gases contribute significantly (Fig. 3.2). Except for the region between $8\text{ }\mu\text{m}$ and $12\text{ }\mu\text{m}$, the atmosphere is nearly opaque to terrestrial radiation. The key absorption features for terrestrial radiation are a water-vapor vibration–rotation band near $6.3\text{ }\mu\text{m}$, the $9.6\text{-}\mu\text{m}$ band of ozone, the $15\text{-}\mu\text{m}$ band of carbon dioxide, and the dense rotational bands of water vapor that become increasingly important at wavelengths longer than $12\text{ }\mu\text{m}$.

Visible radiation is too energetic to be absorbed by most of the gases in the atmosphere and not energetic enough to photodissociate them, so that the atmosphere is almost transparent to it. Solar radiation with wavelengths between about $0.75\text{ }\mu\text{m}$ and $5\text{ }\mu\text{m}$, which we will call near-infrared radiation, is absorbed weakly by water, carbon dioxide, ozone, and oxygen (Fig. 3.1). Most of the ultraviolet radiation from the Sun with wavelengths shorter than $0.2\text{ }\mu\text{m}$ is absorbed in the upper atmosphere through the photodissociation and ionization of nitrogen and oxygen. Radiation at frequencies between $0.2\text{ }\mu\text{m}$ and $0.3\text{ }\mu\text{m}$ is absorbed by ozone in the stratosphere.

3.6 THE LAMBERT–BOUGUER–BEER LAW: FORMULATION OF FLUX ABSORPTION

In Section 3.5, the physical processes whereby molecules absorb and emit radiation were discussed. This section and the following one illustrate how knowledge of the absorption properties of the atmosphere can be incorporated into a formula to calculate the flux of radiation. To simplify the initial discussion, we will not consider emission by the atmosphere. Suppose, for example, that we are interested in the absorption of solar radiation in the atmosphere. Atmospheric gases can absorb solar radiation, but because the atmosphere is much colder than the Sun, the energy reemitted from the atmospheric gases is at longer wavelengths. For the moment, we will ignore scattering and consider that the atmosphere can only transmit or absorb solar radiation.

For many applications, the plane-parallel approximation is accurate and greatly simplifies radiative transfer calculations. Under this approximation the sphericity of Earth is ignored and atmospheric properties are assumed to be functions only of the vertical coordinate. This situation is illustrated in Fig. 3.7. Since incoming solar radiation can be considered to be a parallel beam of radiation, we need consider only one direction of radiation, which is characterized fully in this case by the zenith angle θ .

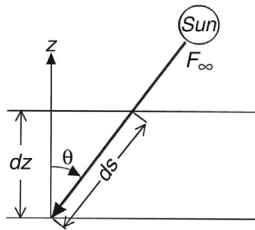


FIGURE 3.7 The extinction path of a solar beam through a plane-parallel atmosphere.

The *Lambert–Bouguer–Beer law of extinction* states that absorption is linear in the intensity of radiation and the absorber amount. The absorption by a layer of depth dz is proportional to the irradiance (F) times the mass of absorber along the path the radiation follows. The proportionality constant derives from the quantum-mechanical considerations outlined in [Section 3.5](#), which determine the probability that a photon with a particular energy will be absorbed by a particular molecule. We call this constant the absorption coefficient and give it the symbol k_{abs} . In general, it depends on the pressure and temperature, since these affect the strength and shape of the absorption lines of the absorber in question.

The change in the irradiance (dF) along a path of length ds , where the density of the absorber is ρ_a and the absorption coefficient is k_{abs} , may be written

$$dF = -k_{\text{abs}} \rho_a F ds \quad (3.12)$$

In (3.12), F and ds are both measured positive downward. F and k_{abs} depend on frequency, but we have dropped the frequency subscript for economy. The units of k_{abs} in (3.12) must be $\text{m}^2 \text{ kg}^{-1}$. Because its units are area per unit mass, k_{abs} is sometimes also called the absorption cross-section of the gas in question. From [Fig. 3.7](#), the path length is related to altitude according to

$$dz = -\cos \theta ds \quad (3.13)$$

Therefore, (3.12) becomes

$$\cos \theta \frac{dF}{dz} = k_{\text{abs}} \rho_a F \quad (3.14)$$

We can define the optical depth (τ) along a vertical path.

$$\tau = \int_z^\infty k_{\text{abs}} \rho_a dz \quad (3.15)$$

Note that (3.15) implies that $d\tau = -k_{\text{abs}} \rho_a dz$, so that we can write (3.14) as

$$\cos \theta \frac{dF}{d\tau} = -F \quad (3.16)$$

This equation has a very simple solution,

$$F = F_\infty e^{-\tau/\cos \theta} \quad (3.17)$$

where F_∞ is, in this case, the downward irradiance at the top of the atmosphere. Thus, the incident radiation decays exponentially along the slant path ds where the optical depth is given by $\tau/\cos \theta$.

3.6.1 Absorption Rate

In an isothermal atmosphere in hydrostatic balance, the density (ρ_a) of an absorber with constant mass-mixing ratio is given by (Section 1.4):

$$\rho_a = \rho_{\text{as}} e^{(-z/H)} \quad (3.18)$$

Here $H = RT/g$ is the scale height, $R = 287 \text{ J K}^{-1} \text{ kg}^{-1}$, $g = 9.81 \text{ ms}^{-2}$, and ρ_{as} is the density of the absorber at the surface. If we introduce this into the equation for optical depth (3.15), assume that k_{abs} is a constant, and perform the integration, we obtain

$$\tau = \frac{p_s}{g} M_a k_{\text{abs}} e^{-z/H} \quad (3.19)$$

where $M_a = \rho_a / \rho$ is the mass mixing ratio of the absorber. From (3.19) we can see that the total optical depth is $(p_s/g)M_a k_{\text{abs}}$, which is the total mass of the absorber per square meter times the absorption cross-section. We can use (3.19) to show that

$$\frac{d\tau}{dz} = -\frac{\tau}{H} \quad (3.20)$$

To calculate the energy absorption rate per unit volume, we multiply the irradiance times the density times the absorption coefficient. Using (3.14), (3.17), and (3.20), and defining $\mu = \cos \theta$, we obtain that

$$\text{Absorption rate} = \frac{dF}{dz} = \frac{k_{\text{abs}} \rho_a F}{\mu} = -\frac{d\tau}{dz} \frac{F}{\mu} = \frac{F_\infty}{\mu} e^{-\tau/\mu} \frac{\tau}{H} \quad (3.21)$$

The absorption rate per unit volume peaks where the product of irradiance and absorbing mass cross-section reaches a maximum. We can find this point by differentiating the absorption rate in (3.21) with respect to optical depth and setting the derivative to zero to find the maximum.

$$\frac{d}{d\tau} \left[\frac{F_\infty}{\mu} e^{-\tau/\mu} \frac{\tau}{H} \right] = \frac{F_\infty}{\mu H} e^{-\tau/\mu} \left[1 - \frac{\tau}{H} \right] = 0 \quad (3.22)$$

Thus, we derive that the absorption rate peaks at $\tau/\mu = 1$. One may show that the pressure level, where the absorption rate per unit volume is maximum, is given by

$$\frac{p_{\max\text{abs}}}{p_s} = \frac{\cos \theta}{H k_{\text{abs}} \rho_{\text{as}}} \quad (3.23)$$

where p_s is the surface pressure. The pressure of maximum absorption is proportional to the cosine of the solar zenith angle, so that as the Sun moves toward the horizon the absorption occurs higher in the atmosphere. The pressure at the level of maximum absorption is inversely proportional to the mass of absorber per unit surface area, $H\rho_{\text{as}}$, and to the absorption coefficient k_{abs} .

The heating rate associated with absorption of a downward flux of radiant energy is given by

$$\left. \frac{\partial T}{\partial t} \right|_{\text{rad}} = \frac{1}{c_p \rho} \frac{\partial F}{\partial z} \quad (3.24)$$

where c_p is the specific heat at constant pressure and ρ is the air density. Utilizing (3.14), (3.24) can be written as

$$\left. \frac{\partial T}{\partial t} \right|_{\text{rad}} = \frac{k_{\text{abs}} M_a}{c_p \mu} F \quad (3.25)$$

If the mass mixing ratio of the absorber, M_a , is independent of altitude, then the heating rate will be proportional to the irradiance itself, which is maximum at the outer extremity of the atmosphere. This is the case for absorption of ultraviolet radiation by molecular oxygen and nitrogen in the upper atmosphere, which produces maximum heating rates at very high altitudes and accounts for the rapid increase of temperature with altitude in the thermosphere shown in Fig. 1.2. For an absorber such as ozone, whose mixing ratio peaks sharply in the stratosphere, the heating rate will also peak in the stratosphere. This local maximum in the ozone-heating rate produces the local maximum in the climatological temperature at the stratopause near 50 km.

3.7 INFRARED RADIATIVE TRANSFER EQUATION: ABSORPTION AND EMISSION

We will further develop the radiative transfer equation for a plane, parallel atmosphere in which both emission and absorption by gases occur. The goal of this section is to provide an intuitive understanding of the transfer of longwave radiation through the atmosphere and its importance for climate. Toward this end, some simplifications will be made that cannot be made in accurate calculations of radiative transfer. Readers not interested in the details of infrared radiative transfer in the atmosphere may skip ahead to [Sections 3.8 and 3.9](#), where simple heuristic models are described. In [Section 3.10](#) the results of more accurate calculations will be presented.

We again make the plane, parallel atmosphere approximation under which Earth is considered to be a flat plane, and the properties of the atmosphere depend only on altitude. These are good approximations if the properties of the atmosphere vary slowly in the horizontal compared to the vertical. This is generally true for temperature and humidity because the atmosphere is so thin compared to the radius of Earth. It may not be a good approximation when clouds are present whose horizontal dimension is comparable to their vertical dimension.

3.7.1 Schwarzschild's Equation

Consider the situation depicted in [Fig. 3.8](#) in which a beam of intensity I_v passes upward through a layer of depth dz , making an angle of θ with the vertical direction. The change of intensity along the path through this layer will be equal to the emission from the gas along the path minus the absorption

$$dI_v = E_v - A_v \quad (3.26)$$

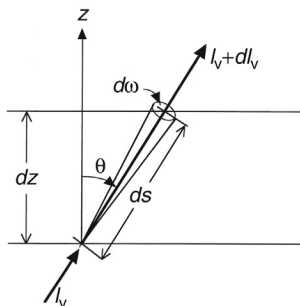


FIGURE 3.8 The path of upward-directed terrestrial radiance through a plane-parallel atmosphere.

The absorption can be assumed to follow the Lambert–Bouguer–Beer law.

$$dI_v = E_v - \rho_a ds k_v I_v \quad (3.27)$$

The emissivity ε_v is defined as the ratio of the emission of a substance to the intensity of radiation in a cavity at equilibrium. The latter is given by *Planck's function* (3.7), so that the emission may be written as follows:

$$E_v = \varepsilon_v B_v(T) \quad (3.28)$$

When collisions with other molecules are much more frequent than radiative transitions of a molecule, the assumption of local thermodynamic equilibrium may be made. This assumption is warranted for most absorption lines in the relatively high-pressure environment of the troposphere and stratosphere. In thermodynamic equilibrium, according to Kirchhoff's law, the emissivity of a substance must be equal to its absorptivity.

With the assumption of local thermodynamic equilibrium, we have $\varepsilon_v = \rho_a ds k_v$ so that (3.27) becomes

$$dI_v = \rho_a ds k_v (B_v(T) - I_v) \quad (3.29)$$

Utilizing $dz = \cos\theta ds$ and taking the limit of small dz , we obtain a radiative transfer equation

$$\cos\theta \frac{dI_v}{dz} = \rho_a k_v (B_v(T) - I_v) \quad (3.30)$$

In this equation, I_v is a function of both altitude z and zenith angle θ , and all other dependent variables are functions of only z . For infrared radiation, we may reasonably assume that the intensity is independent of azimuth angle, φ (Fig. 3.1), and that the blackbody emission, $B_v(T(z))$, is isotropic, being independent of both θ and φ , but still dependent on z .

To proceed toward a solution of (3.30) we again introduce the optical depth, defined this time from the surface ($z = z_s$) upward.

$$\tau_v(z) = \int_{z_s}^z \rho_a k_v dz \quad (3.31)$$

Using the definition (3.31) in (3.30) we obtain

$$\cos\theta \frac{dI_v(\tau_v(z), \theta)}{d\tau_v} = B_v(T(\tau_v(z))) - I_v(\tau_v(z), \theta) \quad (3.32)$$

Parentheses in (3.32) show the dependence of the radiance on zenith angle and altitude, the latter being represented parametrically by vertical optical depth.

Multiply (3.32) by the integrating factor $e^{\tau_v/\mu}$, where $\mu = \cos \theta$, to convert it to a form that can be integrated directly.

$$\mu \frac{d}{d\tau_v} \{I_v(\tau_v(z), \theta) e^{(\tau_v(z)/\mu)}\} = B_v(T(\tau_v(z))) e^{(\tau_v(z)/\mu)} \quad (3.33)$$

We integrate (3.33) from the surface, where the optical depth is zero, to some arbitrary altitude where we wish to calculate the upward intensity and where the optical depth is $\tau_v(z)$. The integral is performed using τ'_v as the dummy variable of integration.

$$I_v(\tau_v(z), \mu) = I_v(0, \mu) e^{-\tau_v(z)/\mu} + \int_0^{\tau_v(z)} \mu^{-1} B_v(T(\tau'_v)) e^{((\tau'_v - \tau_v(z))/\mu)} d\tau'_v \quad (3.34)$$

The first term on the right in (3.34) represents the emission from the surface, reduced by the extinction along the path from the surface to the altitude z . The second term represents the summation of the emissions from all of the layers of the atmosphere below the level z , each reduced by the absorption by the atmosphere between the level of emission and the level z .

3.7.2 Simple Flux Forms of the Radiative Transfer Equation Solution

Simplified flux forms of the solution (3.34) can be derived that yield easier understanding of how fluxes of thermal infrared radiation in the atmosphere depend on the vertical temperature profile and the infrared opacity of the atmosphere. A number of approximations are necessary to derive the following simplified equations for the upward $F^\uparrow(z)$ and downward $F^\downarrow(z)$ terrestrial irradiance at some height z in the atmosphere.

$$F^\uparrow(z) = \sigma T_s^4 \mathcal{T}\{z_s, z\} + \mathcal{T} \int_{\mathcal{T}\{z_s, z\}}^1 \sigma T(z')^4 d\mathcal{T}\{z', z\} \quad (3.35)$$

$$F^\downarrow(z) = \int_{\mathcal{T}\{z, \infty\}}^1 \sigma T(z')^4 d\mathcal{T}\{z', z\}. \quad (3.36)$$

These equations represent the fluxes of terrestrial radiant energy at all frequencies and integrated over all angles in the upward or downward hemispheres, and would be given in Wm^{-2} (Watts per square meter). The fluxes depend on the temperature and on the flux transmission, $\mathcal{T}\{z', z\}$, which is the fraction of the total terrestrial energy flux that can

pass between altitudes z and z' without absorption. The transmission is always between zero, which indicates no transmission, and one, which indicates complete transmission. The transmission approaches one as the two altitudes get arbitrarily close together. As the two altitudes move apart, the transmission decreases at a rate that depends on the absorber amount between them.

The first term on the right in (3.35) is a boundary term and assumes that the ground emits like a blackbody at the temperature of the surface T_s . At the level z the flux density associated with the surface emission is reduced to the fraction $\mathcal{T}\{z_s, z\}$ of its surface value. The integral in (3.35) represents the contribution to the upward flux from the atmosphere below the level z , and in (3.36), the integral represents the contribution to the downward flux at z from the atmosphere above that level. The contributions to these integrals are greatest where the transmission function is changing most rapidly. This occurs when the difference in optical depth between the two locations is close to one.

The net flux of terrestrial radiation is given by the difference between the upward and downward flux:

$$F(z) = F^\uparrow(z) - F^\downarrow(z) \quad (3.37)$$

The heating rate associated with the divergence of the terrestrial flux density is then

$$\frac{\partial T}{\partial t} = -\frac{1}{\rho c_p} \frac{\partial F}{\partial z} \quad (3.38)$$

Of particular interest for climate are the upward flux of terrestrial radiation at the top of the atmosphere and the downward flux at the surface. From (3.35) and (3.36) these are

$$F^\uparrow(\infty) = \sigma T_s^4 \mathcal{T}\{z_s, \infty\} + \int_{\mathcal{T}\{z_s, \infty\}}^1 \sigma T(z')^4 d\mathcal{T}\{z', \infty\} \quad (3.39)$$

$$F^\downarrow(z_s) = \int_{\mathcal{T}\{z_s, \infty\}}^1 \sigma T(z')^4 d\mathcal{T}\{z', z_s\}. \quad (3.40)$$

Figure 3.9 illustrates what the two transmission functions in (3.39) and (3.40) might look like, together with a representation of the temperature profile in the atmosphere. The primary contributions to the integrals come from the levels where the transmission functions are changing most rapidly. In the case of outgoing longwave radiation (OLR), $F^\uparrow(\infty)$, only a small amount of the emission from the surface is able to escape to space under average terrestrial conditions. Under typical conditions, most of the OLR originates in the troposphere at levels where the temperature is significantly less than the surface value. From (3.39)

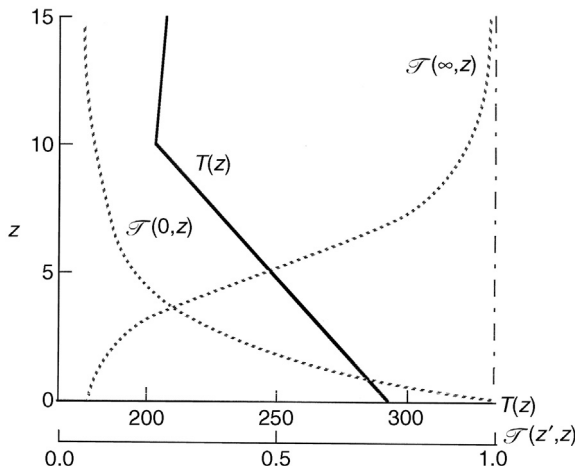


FIGURE 3.9 Transmission functions and air temperature $T(z)$ as functions of altitude.

it can be seen that the emission temperature defined in Chapter 2 is a weighted mean of the temperature profile from the surface to the top of the atmosphere, where the weight is the rate at which the transmission function changes with height.

When an absorbing atmosphere is present, the average emission temperature is less than the surface value, and the loss of energy by emission to space is much less than the infrared emission from the surface. This is one component of the greenhouse effect. Another aspect is the supply of energy to the surface by downward emission of terrestrial radiation from the atmosphere. The downward flux of terrestrial radiation at the surface originates in the lower troposphere, where most of the water vapor resides. The temperatures there are relatively warm. In the global mean, this downward flux is larger by nearly a factor of two than the input of energy to the surface from the Sun (Fig. 2.4).

It is interesting to consider the case of an isothermal atmosphere at temperature T_A , overlying a surface of temperature T_s . In this case, the temperature can be taken outside the integrals in (3.39) and (3.40).

$$F^\uparrow(\infty) = \sigma T_s^4 \mathcal{T}\{z_s, \infty\} + \sigma T_A^4 (1 - \mathcal{T}\{z_s, \infty\}) \quad (3.41)$$

$$F^\downarrow(z_s) = \sigma T_A^4 (1 - \mathcal{T}\{z_s, \infty\}) \quad (3.42)$$

From these expressions we obtain the limiting cases for an opaque and a transparent atmosphere:

$$\mathcal{T}\{z_s, \infty\} = 0 \Rightarrow F^\downarrow(z_s) = \sigma T_A^4, \quad F^\uparrow(\infty) = \sigma T_A^4 \quad (3.43)$$

$$\mathcal{T}\{z_s, \infty\} = 1 \Rightarrow F^\downarrow(z_s) = 0, \quad F^\uparrow(\infty) = \sigma T_s^4 \quad (3.44)$$

In the first limit (3.43) the atmosphere is perfectly opaque to longwave radiation and emits both upward and downward like a blackbody. In this case, the net longwave at the ground is simply related to the difference in blackbody emission by the atmosphere and surface, and the emission to space is entirely from the atmosphere. In the next section, we consider a model atmosphere made up of layers that are opaque to longwave radiation. In the case of perfect transmissivity equal to one (3.44) the atmosphere has no effect on terrestrial radiation, so that the downward longwave is zero and the surface emission escapes directly to space.

Clouds strongly affect the transmission of terrestrial radiation through the atmosphere. If a cloud is reasonably thick and has a sharp top and bottom, then it can be treated accurately as a perfect absorber of longwave radiation. If such a cloud is present with a bottom at z_{cb} and a top at z_{ct} , then (3.39) and (3.40) are changed.

$$F^\uparrow(\infty) = \sigma T_{z_{ct}}^4 \mathcal{T}\{z_{ct}, \infty\} + \int_{\mathcal{T}\{z_{ct}, \infty\}}^1 \sigma T(z')^4 d\mathcal{T}\{z', \infty\} \quad (3.45)$$

$$F^\downarrow(z_s) = \sigma T_{z_{cb}}^4 \mathcal{T}\{z_{cb}, z_s\} + \int_{\mathcal{T}\{z_{cb}, z_s\}}^1 \sigma T(z')^4 d\mathcal{T}\{z', z_s\} \quad (3.46)$$

In this case, the downward flux at the ground (3.46) also has a boundary term coming from the bottom of the cloud. It can be shown using the mean value theorem of calculus that if the temperature decreases with altitude, then a cloud will decrease the outgoing flux at the top of the atmosphere, and increase the downward flux at the ground. The amount of the change will depend on the lapse rate and the position of the cloud top and base relative to the transmission function for the clear atmosphere.

3.8 HEURISTIC MODEL OF RADIATIVE EQUILIBRIUM

A layer of atmosphere that is almost opaque for longwave radiation can be crudely approximated as a blackbody that absorbs all terrestrial radiation that is incident upon it and emits like a blackbody at its temperature. For an atmosphere with a large infrared optical depth, the radiative transfer process can be represented with a series of blackbodies arranged in vertical layers. Two layers centered at 0.5 km and 2.0 km altitudes provide a simple approximation for Earth's atmosphere. If we assume that the

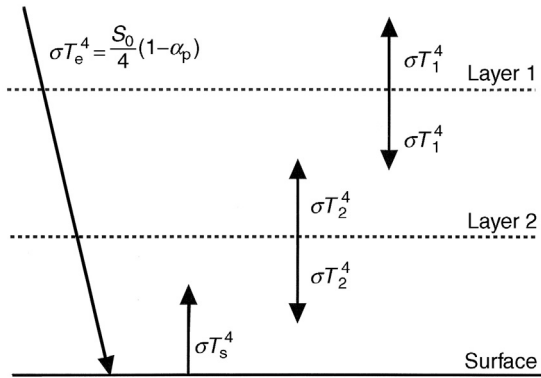


FIGURE 3.10 Simple two-layer radiative equilibrium model for the atmosphere–earth system, showing the fluxes of radiant energy.

atmospheric layers are transparent to solar radiation, we have the schematic energy flow diagram shown in Fig. 3.10.

We can solve for all of the unknown temperatures by using the energy balance at each of the layers. If no net energy gain or loss occurs at any of the levels, then the temperatures obtained are the radiative equilibrium values. At the top of the atmosphere we must have energy balance, so that

$$\frac{S_0}{4}(1-\alpha_p) = \sigma T_e^4 = \sigma T_1^4 \quad (3.47)$$

We thus know immediately that the top layer temperature must equal the emission temperature of the planet, since, in this approximation, the only longwave emission that escapes to space comes from the upper layer. The energy balance at layer 1 is

$$\sigma T_2^4 = 2\sigma T_1^4 \quad (3.48)$$

The balance at layer 2 yields

$$\sigma T_1^4 + \sigma T_s^4 = 2\sigma T_2^4 \quad (3.49)$$

And the balance at the surface is

$$\frac{S_0}{4}(1-\alpha_p) + \sigma T_2^4 = \sigma T_s^4 \quad (3.50)$$

The critical effect of an atmosphere that absorbs and emits longwave radiation appears in (3.50). The energy supplied to the surface by the Sun is augmented by a downward flux of longwave radiation from the

atmosphere. This allows the surface temperature to rise significantly above the value it would have in the absence of an atmosphere.

We can use (3.47) through (3.50) to solve for the surface temperature.

$$T_s^4 = 3 \frac{(S_0 / 4)(1 - \alpha_p)}{\sigma} = 3T_e^4 \quad (3.51)$$

By extension, if such a model atmosphere has an arbitrary number of layers, n , the surface temperature in equilibrium will be

$$T_s = \sqrt[4]{n+1} T_e$$

The radiative equilibrium surface temperature for a two-layer atmosphere is 335 K, which is much hotter than Earth's surface temperature. Radiative equilibrium is not a good approximation for the surface temperature, since we know that latent and sensible heat fluxes remove substantial amounts of energy from the surface and drive a lapse rate that is less than the radiative equilibrium lapse rate.

If the atmosphere absorbs no solar radiation, for a thin layer of emissivity ε near the top of the atmosphere, the energy balance is between absorption of the flux of terrestrial radiation from below and the emission from the layer itself.

$$\varepsilon\sigma T_e^4 = 2\varepsilon\sigma T_{\text{strat}}^4 \quad (3.52)$$

where T_{strat} is the temperature at the outer edge of the atmosphere, which we may take to be the stratosphere.

A thin layer of atmosphere near the surface absorbs a fraction ε of the emission from above and below and emits in both directions. The temperature of the air adjacent to the surface, T_{SA} , may be derived from the energy balance there.

$$\varepsilon\sigma T_s^4 + \varepsilon\sigma T_2^4 = 2\varepsilon\sigma T_{\text{SA}}^4 \quad (3.53)$$

We can solve for all of the temperatures and obtain the following values.

$$T_1 = 255 \text{ K} \quad T_2 = 303 \text{ K} \quad T_s = 335 \text{ K}$$

$$T_{\text{strat}} = 214 \text{ K} \quad T_{\text{SA}} = 320 \text{ K}$$

These temperatures are plotted in Fig. 3.11. In pure radiative equilibrium, the temperatures of the surface and the air in contact with the surface are different. This discontinuity is caused by the absorption of solar radiation at the surface. Such discontinuities are usually greatly suppressed in reality because of efficient heat transport by conduction and convection.

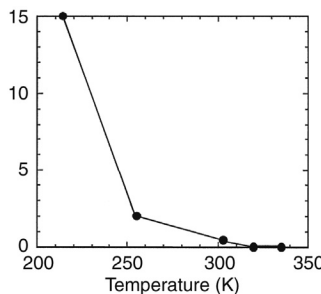


FIGURE 3.11 Plot of the vertical temperature profile obtained from the simple two-level atmosphere radiative equilibrium model.

Note that the lapse rate is much greater than the dry adiabatic lapse rate of 9.8 K km^{-1} , dropping by 80 K in the lowest 2 km, so that the radiative equilibrium temperature profile is unstable and any small motion will induce growth of convection.

3.9 CLOUDS AND RADIATION

Clouds consist of liquid water droplets or ice particles suspended in the atmosphere. They are formed by the condensation of atmospheric water vapor when the temperature falls below the saturation temperature. Water droplets and ice particles have substantial interactions with both solar and terrestrial radiation (Fig. 3.12). The nature of these interactions

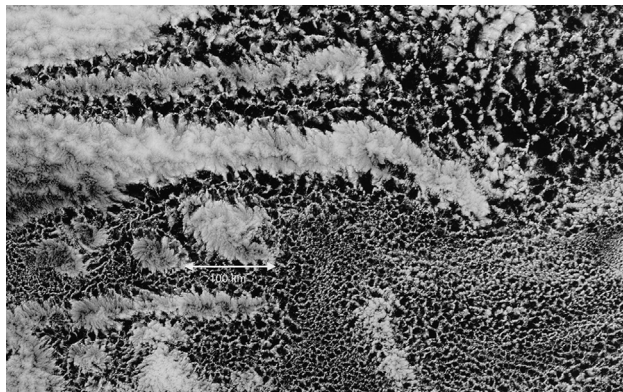


FIGURE 3.12 Stratocumulus clouds in the southeast tropical Pacific Ocean. Cells and structures of many scales are present. Some cells are closed and bright, while others are open and dark, revealing the lower albedo of the underlying ocean. *NASA MODIS Aqua image, April 17, 2010.*

depends on the total mass of water, the size and shape of the droplets or particles, and their distribution in space. The problem is often simplified by assuming that clouds are uniform and infinite in the horizontal, which is called the plane-parallel cloud assumption. If the droplet size distribution and the vertical distribution of humidity are assumed, then the cloud albedo and absorption depend on the total liquid water content of the cloud and the solar zenith angle. Cloud liquid water content is defined as the total mass of cloud water in a vertical column of atmosphere per unit of surface area.

For a particle of radius r the amount by which it reduces an incident beam of radiation I_0 is $\pi r^2 k_e I_0$, where k_e is the extinction efficiency. In general, this extinction will be composed of extinction by scattering and extinction by absorption, so that $k_e = k_s + k_a$. The optical depth for a layer of particles of depth h can be written

$$\tau = \pi h \int_0^\infty k_e(r) r^2 n(r) dr \quad (3.54)$$

where $n(r)$ is the number density of particles of radius r . For particles that are large compared to the wavelength of radiation the extinction efficiency $k_e \approx 2$. If the distribution of particle radii is peaked near an average value \bar{r} , then one can write approximately that,

$$\tau = 2\pi h \bar{r}^2 N \quad (3.55)$$

where $N = \int_0^\infty n(r) dr$ is the total particle density and h is the depth of the cloud. For a water cloud, the total mass of liquid water per unit surface area of the cloud (LWC) is

$$LWC = \frac{4}{3} \pi \bar{r}^3 \rho_L h N \quad (3.56)$$

where ρ_L is the density of water and h is the depth of the cloud. Combining (3.55) and (3.56) the optical depth can be expressed as

$$\tau = \frac{3}{2} \frac{LWC}{\rho_L \bar{r}} \quad (3.57)$$

So for fixed liquid water content, the optical depth of the cloud varies inversely with the average particle radius. This is because refraction of light occurs at the interface between water and air, and smaller particles have a larger ratio of surface area to volume (and mass) than larger particles. Humans can potentially alter the clouds by releasing extra cloud condensation nuclei, the particles on which cloud droplets preferentially form. With more condensation nuclei, the water is spread over more droplets and the average radius decreases, brightening the clouds.

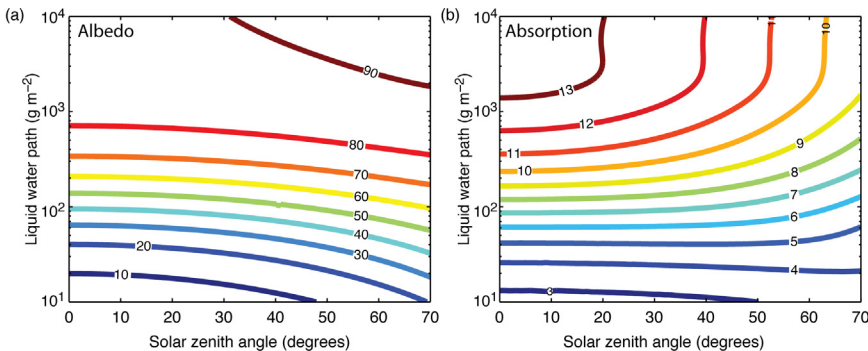


FIGURE 3.13 The dependence of (a) cloud albedo and (b) cloud absorption on cloud liquid water path and solar zenith angle calculated for plane parallel clouds. Values are given in percent. Calculation is for a cloud above a nonreflective surface and an effective radius of the cloud droplets of $14 \mu\text{m}$ was used.

Model calculations of the cloud albedo and absorption for plane-parallel water clouds are shown in Fig. 3.13. The albedo increases with the total water content or depth of the cloud and also with the solar zenith angle. The albedo increase with liquid water content is most rapid for smaller amounts of liquid water. As the cloud becomes very thick, the cloud albedo slowly approaches a limiting upper value and becomes insensitive to further increases in cloud mass. In very thick clouds, most of the solar radiation is scattered before it can reach the particles deep in the cloud, and radiation that is scattered from particles deep in the cloud is unlikely to find its way back out to space. For these reasons, increases in the optical thickness of a cloud eventually cease to make much difference in the reflectivity of the cloud. The variation of albedo with zenith angle is most rapid when the Sun is near the horizon, and least when the Sun is overhead. Absorption of solar radiation by plane-parallel clouds decreases with increasing zenith angle because radiation that is reflected to space at the higher zenith angles penetrates less deeply into the cloud and is therefore less likely to be absorbed. The absorption increases with liquid water content for an overhead sun, but the fraction absorbed is always much less than the fraction reflected.

The variations of the albedo of typical clouds in the atmosphere are dominated by the column amount of liquid water and ice in the cloud. Nonetheless, the albedo of clouds is sensitive to the droplet size as suggested by (3.57). Figure 3.14 shows how the calculated albedo of clouds changes as the radius of the droplets is varied, while keeping the liquid water content fixed. The albedo is greatest for smaller droplets, principally because these present a larger surface area for the same mass.

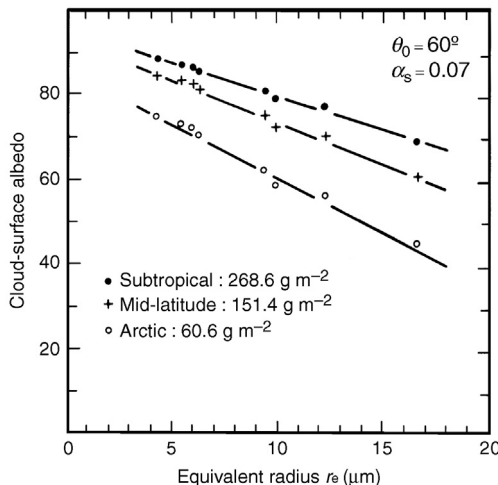


FIGURE 3.14 The dependence of planetary albedo on the size of cloud droplets. From Slingo and Schrecker (1982). Reprinted with permission from the Royal Meteorological Society.

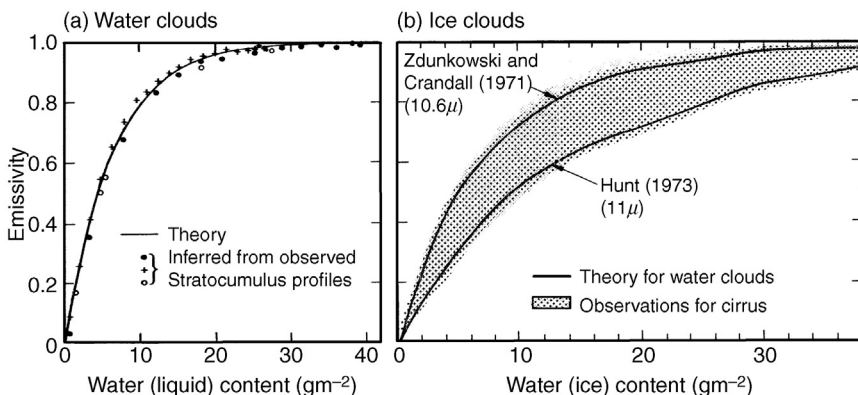


FIGURE 3.15 The dependence of the longwave emissivity on (a) liquid water content and (b) ice content. (a) Slingo et al. (1982); reprinted with permission from the Royal Meteorological Society (b) Griffith et al. (1980); reprinted with permission from the American Meteorological Society.

Clouds absorb terrestrial radiation very effectively. Figure 3.15 shows the emissivity of water and ice clouds as a function of liquid water content. Clouds become opaque to longwave radiation when the liquid water path exceeds about 20 gm^{-2} . If this liquid water path is achieved in an altitude range where the temperature is essentially uniform, then cloud surfaces can be assumed to absorb and emit terrestrial radiation essentially like black-bodies with the temperature at the edge of the cloud. This assumption is

a good one except for thin clouds such as cirrus, which may be partially transparent to longwave radiation. Comparison of Figs. 3.13 and 3.15 shows that the albedo of clouds continues to increase with additional liquid water content long after the cloud has become opaque to longwave radiation.

3.10 RADIATIVE–CONVECTIVE EQUILIBRIUM TEMPERATURE PROFILES

As a reasonably straightforward method of attempting to understand the effects of radiative transfer on climate, one can solve the radiative transfer equation for global mean terrestrial conditions. This involves construction of appropriate models for the transmission of the various band systems of importance in the atmosphere, insertion of these into a computational analog of the radiative transfer equation, and iteration to obtain a steady balance solution. Such models are a much more sophisticated version of the simple radiative equilibrium model discussed in Section 3.8.

The variables that determine the fluxes of radiant energy in the atmosphere include the atmospheric gaseous composition, the aerosol and cloud characteristics, the surface albedo, and the insolation. Since horizontal transport of energy by atmospheric and oceanic motion affects the local climate, it is simplest to calculate the radiative equilibrium for conditions averaged over the globe. In a global-mean model the temperature and all other variables depend only on altitude, and the globally averaged insolation and solar zenith angle are appropriate. To understand the basic radiative energy balance of Earth, we need to specify the following:

1. H_2O : Water vapor is the most important gas for the transfer of radiation in the atmosphere. Its distribution is highly variable. The sources and sinks (evaporation and condensation) are determined by the climate itself, and they are fast compared to the rate at which the atmosphere's motion mixes moist and dry air together. Water vapor has a vibration–rotation band near $6.3\text{ }\mu\text{m}$ and a large number of closely spaced rotation lines at wavelengths longer than about $12\text{ }\mu\text{m}$. It is also the principal absorber of solar radiation in the troposphere. Since the saturation vapor pressure of water is very sensitive to temperature, the relative humidity is sometimes specified in calculations, rather than the absolute humidity, when the humidity cannot be directly solved for. This allows the water-vapor feedback to be simulated in the model.
2. CO_2 : The mixing ratio of carbon dioxide is increasing about 2 ppmv per year primarily because of fossil fuel combustion. In 2014 the value was about 400 ppmv, compared to a value in 1750 of about 280 ppmv. Because sources and sinks of CO_2 are slow compared to the time it takes the atmosphere to mix thoroughly, its mixing ratio is

approximately constant with latitude and altitude up to about 100 km. The strong vibration–rotation band of CO₂ at 15 μm is important for longwave radiative transfer. A significant amount of solar radiation is also absorbed by carbon dioxide.

3. O₃: Ozone has fast sources and sinks in the stratosphere where most of the atmospheric ozone resides. Near the surface, ozone is produced in association with photochemical smog. Its concentration in the middle and upper stratosphere is dependent on temperature, ultraviolet radiation, and a host of photochemically active trace species. Ozone has a vibration–rotation band near 9.6 μm that is important for longwave energy transfer, and also has a dissociation continuum that absorbs solar radiation between 200 nm and 300 nm, which protects life from harmful ultraviolet radiation. Absorption of solar radiation by ozone heats the middle atmosphere and causes the temperature increase with height that defines the tropopause and stratosphere. Stratospheric ozone has decreased because of the chlorine in manmade chemicals. Tropospheric ozone has increased because of human produced pollution, especially nitrous oxides from fuel combustion.
4. *Other greenhouse gases*: Many other atmospheric gases absorb and emit terrestrial radiation and contribute to the greenhouse effect. Many of these are changing in response to human activities. They will be discussed more fully in Chapter 13.
5. *Aerosols*: Atmospheric aerosols of various types affect the transmission of both solar and terrestrial radiation. A layer of sulfuric acid aerosols exists near 25 km in the mid-stratosphere, which increases and decreases in association with volcanic eruptions. Nearer the surface many different types of aerosols are produced by natural and human activities. Some of these absorb solar radiation (e.g., soot) whereas others mostly scatter radiation (e.g., sulfuric acid and organic aerosols).
6. *Surface albedo*: The surface albedo is highly variable from location to location in land areas, depending on the type and condition of the surface material and vegetation (see Chapter 4). Over open ocean the albedo is low but does vary with solar zenith angle and sea state. When the surface is snow covered, its albedo is generally much higher than when surface ice is not present.
7. *Clouds*: Clouds vary considerably in amount and type over the globe. They have very important effects on longwave and solar energy transfer in the atmosphere. The distribution in time and space and the optical properties of clouds are important for climate. For a global-mean radiative equilibrium calculation, cloud radiative properties must be specified. The simplest approach is to assume plane-parallel clouds and specify their distribution in the vertical. The optical properties of the clouds must also be specified. In global warming calculations, clouds must be determined as part of the climate model.

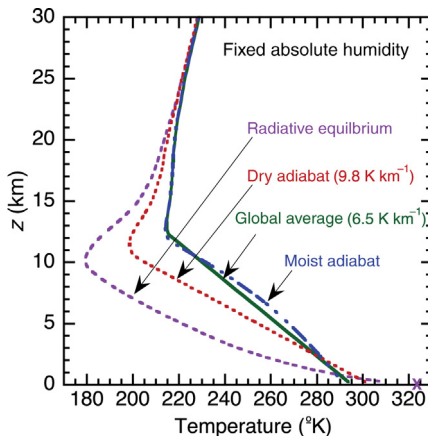


FIGURE 3.16 Calculated temperature profiles for radiative equilibrium, and thermal equilibrium with lapse rates of $9.8^{\circ}\text{C km}^{-1}$, $6.5^{\circ}\text{C km}^{-1}$, and the moist adiabatic lapse rate with clear skies. Absolute humidity, CO_2 (390 ppmv) and ozone have been specified from observations.

Figure 3.16 shows a calculated temperature profile that is in radiative equilibrium. Atmospheric temperatures in radiative equilibrium decrease rapidly with altitude near the surface and, as previously noted, the surface temperature is different from that of the air adjacent to the surface. In the troposphere, radiative equilibrium temperature profiles are hydrostatically unstable in the sense that parcels of air that are elevated slightly will become buoyant and continue to rise. In the real atmosphere, atmospheric motions move heat away from the surface and mix it through the troposphere. Figure 2.4 indicates that 60% of the energy removal from the surface is done by the transport of heat and water vapor by atmospheric motions and only 40% by net longwave radiation emission. The global mean temperature profile of Earth's atmosphere is not in radiative equilibrium, but rather in radiative–convective equilibrium. To obtain a realistic global-mean vertical energy balance, the vertical flux of energy by atmospheric motions must be included.

The simplest method by which the effect of vertical energy transports by motions can be included in a global-mean radiative transfer model is a procedure called *convective adjustment*. Under this constraint the lapse rate is not allowed to exceed a critical value, which must be specified. One can choose the observed global mean value of 6.5 K km^{-1} , or some other value as desired. Where radiative processes would make the lapse rate greater than the specified maximum value, a nonradiative upward heat transfer is assumed to occur that maintains the specified lapse rate while conserving energy. This artificial vertical redistribution of energy is intended to represent the effect of atmospheric motions on the vertical temperature profile without explicitly calculating nonradiative energy fluxes or atmospheric

motions. In a global mean model, this “adjusted” layer extends from the surface to the tropopause.

A temperature profile that is in energy balance when radiative transfer and convective adjustment are taken into account may be called a *radiative–convective equilibrium* or *thermal equilibrium* profile. Thermal equilibrium profiles for assumed maximum lapse rates of $6.5^{\circ}\text{C km}^{-1}$ and the dry adiabatic lapse rate of $9.8^{\circ}\text{C km}^{-1}$ are also shown in Fig. 3.16. The thermal equilibrium profile obtained with a lapse rate of $6.5^{\circ}\text{C km}^{-1}$ is close to the observed global mean temperature profile. No a priori reason exists for choosing a $6.5^{\circ}\text{C km}^{-1}$ adjustment lapse rate other than that it corresponds to the observed global-mean value. However, the assumed lapse rate of $6.5^{\circ}\text{C km}^{-1}$ is close to what is obtained if the moist adiabatic lapse rate is assumed. The maintenance of the lapse rate of the atmosphere is complex and involves many processes and scales of motion. Note that when the chosen lapse rate is larger, the surface temperature increases, when the specific humidity is fixed as a function of pressure. When the lapse rate is increased, the emission from the atmospheric water vapor occurs at a colder temperature relative to the surface, and the surface temperature must increase because of the enhanced greenhouse effect. Because the albedo has not been changed, the emission temperature of the Earth is about the same, roughly where the $6.5^{\circ}\text{C km}^{-1}$ and $9.8^{\circ}\text{C km}^{-1}$ profiles cross.

One use of a climate model is to understand what factors are most important and how changes in these factors will affect the climate. In particular, the one dimensional radiative–convective equilibrium model is useful for understanding the role of trace gases and clouds in determining the temperature profile. Figure 3.17 shows three equilibrium profiles obtained

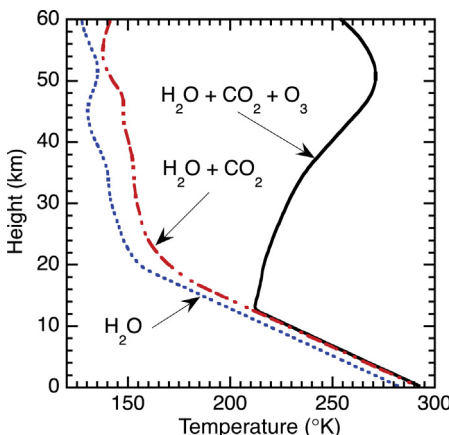


FIGURE 3.17 Thermal equilibrium profiles for three cloudless atmospheres obtained with a critical lapse rate of 6.5 K km^{-1} . One atmosphere has water vapor only; one includes water vapor and carbon dioxide; and the third contains water vapor, carbon dioxide, and ozone.

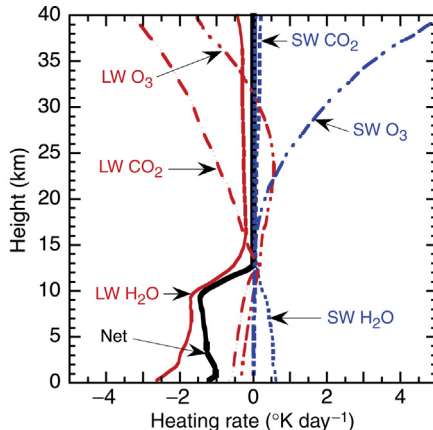


FIGURE 3.18 Radiative heating rate profiles for a clear atmosphere. LWH₂O, LWCO₂, and LWO₃ show the heating rates associated with longwave cooling by water vapor, carbon dioxide, and ozone, respectively. The SW prefix indicates the heating rate associated with solar absorption by each of these gases. Net is the sum of the solar and longwave radiative heating rates contributed by all gases¹.

with different gaseous compositions, but without clouds. With only water vapor present a reasonable approximation to the observed profile is obtained except that the stratosphere is absent. Carbon dioxide with a mixing ratio of 300 ppm raises the temperature about 10 K above the equilibrium obtained with only water vapor present. A sharp tropopause and the increase of temperature with height that characterizes the stratosphere appear only when solar absorption by ozone is included in the model.

The contributions of individual gases to the heating rate in radiative-conductive equilibrium are shown in Fig. 3.18. In the stratosphere, the lapse rate for radiative equilibrium is never large and positive, so convective adjustment is not required. The first-order balance is between heating produced by solar absorption by ozone and cooling produced by longwave emission from carbon dioxide. The troposphere is not in radiative equilibrium, and convective heat transfer from the surface balances a net radiative cooling rate of about 1.5 K day^{-1} . A net positive radiative imbalance exists at the surface. In a clear atmosphere, cooling by water vapor alone provides a good approximation to the net

¹Note that because of overlap between water vapor and carbon dioxide absorption lines, the heating rates in the troposphere do not add up. The contributions were calculated by taking the equilibrium temperature profile and calculating the heating rate for an atmosphere that only contained the gas in question.

longwave cooling. In the troposphere, longwave cooling from carbon dioxide is approximately balanced by solar absorption by water vapor. From the results of radiative–convective equilibrium calculations presented in [Figs. 3.17 and 3.18](#), we conclude that water vapor is by far the preeminent greenhouse gas in the atmosphere for today’s climate. Note that water vapor concentrations vary with temperature, so that processes internal to the climate system adjust water vapor concentrations on short time scales.

3.11 THE ROLE OF CLOUDS IN THE ENERGY BALANCE OF EARTH

It is possible to use Earth-orbiting satellites to accurately measure the radiative fluxes of energy entering and leaving Earth. If the spatial resolution of the measurements of the energy fluxes provided by the instrument on the satellite is great enough, then cloud-free scenes may be identified. These cloud-free scenes can be averaged together to estimate the clear-sky radiation budget. If these cloud-free scenes are taken to represent the atmosphere in the absence of clouds, then the difference between the cloud-free radiation budget and the average of all scenes represents the effect of clouds on the radiation budget. We can call the effect of clouds on the radiation budget the cloud radiative effect on the energy balance. The net cloud radiative effect is the difference between the net radiation at the top of the atmosphere and what the net radiation would be if clouds were removed from the atmosphere leaving all else unchanged.

$$\Delta R_{\text{TOA}} = R_{\text{Average}} - R_{\text{Clear}} \quad (3.58)$$

The net cloud radiative effect can be decomposed into its longwave and shortwave components. Since net radiation is absorbed solar minus outgoing longwave radiation,

$$R_{\text{TOA}} = Q_{\text{abs}} - \text{OLR} \quad (3.59)$$

then

$$\Delta R_{\text{TOA}} = \Delta Q_{\text{abs}} - \Delta \text{OLR} \quad (3.60)$$

The first term on the right is the shortwave cloud effect and the second is the longwave effect. Note that a reduction in OLR is an increase in net radiation.

[Table 3.2](#) shows estimates of the globally and annually averaged radiation budget components for average conditions, cloud-free conditions, and the difference between them. In round numbers, the observations indicate that clouds increase the albedo from 15% to 29%, which results in

TABLE 3.2 Cloud Radiative Effect on the Top-of-Atmosphere Global Energy Balance as Estimated from Satellite Measurements

	Average	Cloud free	Cloud effect
OLR	240	266	+26
Absorbed solar radiation	240	288	-47
Net radiation	+0.56	+22	-21
Albedo	29%	15%	+14%

Irradiances are given in Wm^{-2} and albedo in percent.

From CERES data as described in Loeb *et al.* 2009.

a reduction of absorbed solar radiation of 47 Wm^{-2} . This cooling is offset somewhat by the greenhouse effect of clouds, which reduce the OLR by about 26 Wm^{-2} . The net cloud radiative effect is thus a loss of about 21 Wm^{-2} . The meaning of this number is that, if clouds could suddenly be removed without changing any other climate variable, then Earth would begin to gain 21 Wm^{-2} in net radiation and consequently begin to warm up. Of course clouds are not an external forcing to the climate system, but are rather part of it, and their radiative effects are part of the internal adjustment of the climate. It is important to consider how clouds of different types can affect the energy budget and thereby the temperature.

We can examine how clouds with different properties affect the equilibrium climate using the one-dimensional global thermal equilibrium model explored in the previous section. To do this we consider three simple types of clouds as defined in [Table 3.3](#) and assume that they cover 100% of the Earth. The “average cloud” was chosen to produce the observed global mean effect of clouds on the Earth’s energy balance shown in [Table 3.2](#), and also give a surface temperature near the observed value of 288 K. In reality, the cloud effect on the energy balance is caused by clouds of varying types and characteristics that cover only a portion of the globe.

TABLE 3.3 Cloud Properties Used to Compute [Fig. 3.19](#)

Cloud	Base (km)	Top (km)	L/IWP (gm^{-2})	Particle radius (μm)
Average	2.0	2.5	36	15
Low	2.0	2.5	100	15
High	12.5	13	29	15

L/IWP means the liquid or ice (for high cloud) mass of the cloud.

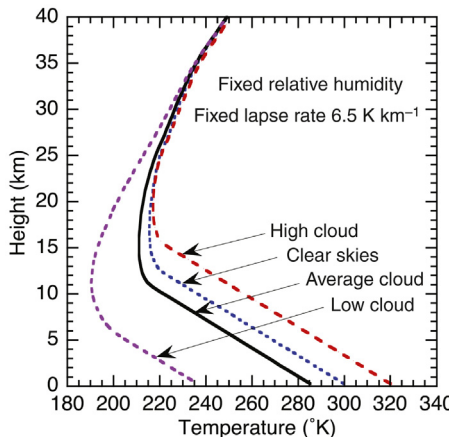


FIGURE 3.19 Thermal equilibrium temperature profiles for atmospheres with various cloud distributions as given in [Table 3.3](#). The lapse rate is constrained to not exceed 6.5 K km^{-1} and the absolute humidity profile is set to approximately the currently observed value.

Here we represent that more complex effect with a single, relatively thin, relatively low cloud that covers 100% of the planet. To contrast with this average cloud we also consider a “high cloud”, with the same albedo as the average cloud but at a higher altitude, and a “low cloud” with a higher albedo at the same altitude as the average cloud.

[Figure 3.19](#) shows the effect on the thermal equilibrium temperature profile of inserting the clouds described in [Table 3.3](#). In these calculations the relative humidity distribution with height is assumed fixed, so that as the climate warms or cools, the water vapor changes. In reality it is more likely that the relative humidity would remain nearly constant and the specific humidity would increase with surface temperature. We will discuss the effects of this later. The average cloud cools the surface compared to clear skies, as expected, since it introduces a negative net change to Earth’s energy balance. Low clouds with high albedos greatly reduce the temperature at the surface and in the troposphere, because they increase the albedo of Earth, but their tops are at low altitudes and high temperatures, so they don’t have a very strong greenhouse warming effect.

The addition of high clouds can cause the surface temperature to exceed the value obtained for both average cloud and cloud-free conditions, since they greatly reduce the outgoing longwave and, if they are relatively thin, do not reduce the absorbed solar radiation by enough to offset the reduced longwave emission. The high cloud specified in [Table 3.3](#) was chosen to produce the same albedo as the average cloud, but because its

TABLE 3.4 Longwave and Shortwave Upward Top-of-Atmosphere Fluxes (Wm^{-2}) and Albedos for the Cases Shown in Fig. 3.19

	LW (up)	SW (up)	Albedo
Clear	291	51	0.15
Average	240	102	0.30
Low	193	149	0.44
High	240	102	0.30

Note how the average cloud and high cloud cases have the same top of atmosphere energy fluxes, but very different temperatures.

top is so high and its greenhouse effect so strong, it causes the surface temperature in equilibrium to be much warmer, even though the net absorbed and emitted radiation are the same as the average cloud case. The OLR, reflected shortwave and albedo for each of the cases shown in Fig. 3.19 are shown in Table 3.4. It is an intriguing aspect of high, thin clouds that they can greatly change the surface temperature in equilibrium without changing the energy balance at the top of the atmosphere. Thus we illustrate that the surface temperature can be very different for the same top-of-atmosphere radiation budget, depending on the types of clouds that the climate produces.

We can also calculate the cloud radiative effect of each of these cloud types. Remember that the cloud radiative effect is the effect on the energy balance of inserting the cloud without changing the temperature or humidity profiles. The numbers in Table 3.5 are obtained by using the temperature profile for the average cloud case shown in Fig. 3.19, and then calculating the top-of-atmosphere energy fluxes with and without each type of cloud. These numbers can be compared to the observed

TABLE 3.5 Cloud Forcing for the Cloud Types in Table 3.2 if inserted into an Atmosphere With the Average-Sky Humidity and Thermal Equilibrium Temperature Profile Shown in Fig. 3.19

	LW (up)	LWCF	SW (up)	SWCF	Net CF
Clear	265	0.0	51	0.0	0.0
Mean	240	24	102	-50	-26
Low	238	27	149	-98	-71
High	125	140	102	-50	+90

LWCF and SWCF are the changes in longwave and shortwave fluxes, respectively, as a result of inserting a cloud into the atmosphere. Net CF is their sum.

values shown in [Table 3.2](#). Because the low cloud has a relatively warm top, its effect on escaping longwave radiation is modest and its net cloud radiative effect is -71 Wm^{-2} . On the other hand, the high cloud has a very cold top and greatly reduces the escaping longwave radiation, so that its net radiative effect is $+90 \text{ Wm}^{-2}$. So the difference in net radiative effect between the high cloud and the low cloud is 161 Wm^{-2} , which is huge.

3.12 A SIMPLE MODEL FOR THE NET RADIATIVE EFFECT OF CLOUDINESS

We can illustrate the relative roles of the reflection of solar radiation and trapping of longwave radiation by clouds with a very simple model of their effect on the global energy balance at the top of the atmosphere. The energy balance at the top of the atmosphere is the difference between the absorbed solar radiation and the outgoing longwave radiation [\(3.59\)](#).

$$R_{\text{TOA}} = \frac{S_0}{4}(1 - \alpha_p) - F^\uparrow(\infty) \quad (3.61)$$

where S_0 is the total solar irradiance and α_p is the albedo, so that $(S_0/4)(1 - \alpha_p) = Q_{\text{abs}}$ is the absorbed solar radiation.

We wish to calculate the difference in the net radiation that results from adding a cloud layer with specified properties to a clear atmosphere.

$$\Delta R_{\text{TOA}} = R_{\text{Cloudy}} - R_{\text{Clear}} = \Delta Q_{\text{abs}} - \Delta F^\uparrow(\infty) \quad (3.62)$$

Suppose that we can specify the albedo for both clear and cloudy conditions, so that the difference in absorbed solar radiation is

$$\begin{aligned} \Delta Q_{\text{abs}} &= \frac{S_0}{4}(1 - \alpha_{\text{Cloudy}}) - \frac{S_0}{4}(1 - \alpha_{\text{Clear}}) \\ &= -\frac{S_0}{4}(\alpha_{\text{Cloudy}} - \alpha_{\text{Clear}}) = -\frac{S_0}{4}\Delta\alpha_p \end{aligned} \quad (3.63)$$

To calculate the change in OLR, we subtract [\(3.39\)](#) from [\(3.45\)](#):

$$\Delta F^\uparrow(\infty) = F^\uparrow_{\text{Cloudy}}(\infty) - F^\uparrow_{\text{Clear}}(\infty) \quad (3.64)$$

$$\Delta F^\uparrow(\infty) = \sigma T_{z_{\text{ct}}}^4 \mathcal{T}\{z_{\text{ct}}, \infty\} - \sigma T_s^4 \mathcal{T}\{z_s, \infty\} - \int_{\mathcal{T}\{z_s, \infty\}}^{\mathcal{T}\{z_{\text{ct}}, \infty\}} \sigma T(z')^4 d\mathcal{T}\{z', \infty\} \quad (3.65)$$

If the top of the cloud is above most of the gaseous absorber of longwave radiation, which is water vapor, then we may make the approximation

$$\mathcal{T}\{z_{\text{ct}}, \infty\} \approx 1.0 \quad (3.66)$$

in which case (3.65) becomes

$$\Delta F^\uparrow(\infty) = \sigma T_{z_{\text{ct}}}^4 - \sigma T_s^4 \mathcal{T}\{z_s, \infty\} - \int_{\mathcal{T}\{z_s, \infty\}}^1 \sigma T(z')^4 d\mathcal{T}\{z', \infty\} \quad (3.67)$$

or

$$\Delta F^\uparrow(\infty) = \sigma T_{z_{\text{ct}}}^4 - F_{\text{Clear}}^\uparrow(\infty) \quad (3.68)$$

Inserting (3.63) and (3.68) into (3.62) gives an approximate formula for the change in net radiation at the top of the atmosphere that is produced by the addition of clouds to a clear atmosphere.

$$\Delta R_{\text{TOA}} = -\frac{S_0}{4} \Delta \alpha_p + F_{\text{Clear}}^\uparrow(\infty) - \sigma T_{z_{\text{ct}}}^4 \quad (3.69)$$

If the cloud top is above most of the longwave absorber, then (3.69) indicates that the change in net radiation produced by the cloud depends on the albedo contrast between clear and cloudy conditions and on the temperature at the cloud top. Since most of the water vapor is in the first few kilometers of the atmosphere, the approximation (3.67) is qualitatively correct for cases with cloud tops above 4 or 5 km.

From (3.69), it is possible that the albedo contrast and the cloud top temperature can be such that the cloud produces no change in the net radiation. The condition for this is obtained by setting $\Delta R_{\text{TOA}} = 0$ in (3.69) and solving for the cloud top temperature.

$$T_{z_{\text{ct}}} = \left\{ \frac{-(S_0 / 4) \Delta \alpha_p + F_{\text{Clear}}^\uparrow(\infty)}{\sigma} \right\}^{1/4} \quad (3.70)$$

If we assume that the temperature decreases with a lapse rate Γ from a surface value of T_s , then the temperature of the cloud top can be related to its altitude.

$$T_{z_{\text{ct}}} = T_s - \Gamma z_{\text{ct}} \quad (3.71)$$

We can use (3.70) and (3.71) to solve for the cloud top altitude for which the reduction in OLR will just cancel the reduction in absorbed solar radiation associated with the presence of a cloud. For numeric values, we can use a solar irradiance of 1360 W m^{-2} , a clear-sky OLR of 265 W m^{-2} , a surface temperature of 288 K , and a lapse rate of 6.5 K km^{-1} . These are all reasonable global-mean values. The resulting curve of cloud top altitude versus albedo contrast is shown as the heavy curve in Fig. 3.20. Clouds with albedo contrasts and altitudes that fall along the heavy line have no

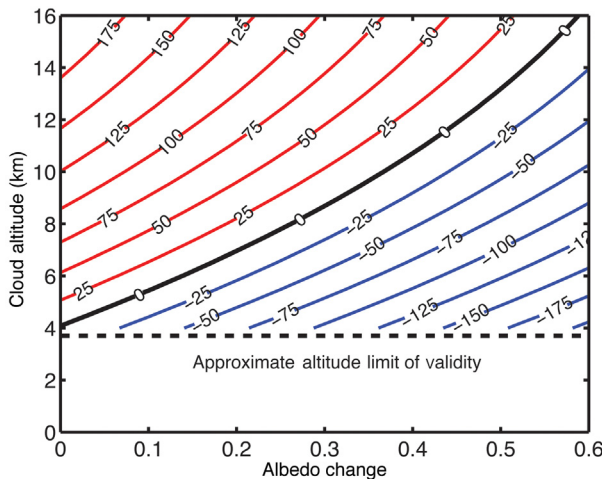


FIGURE 3.20 Contours of change in net radiation at the top of the atmosphere caused by the insertion of a cloud into a clear atmosphere, plotted against cloud top altitude and the planetary albedo contrast between cloudy and clear conditions. The net radiation changes are calculated with the approximate model described in Section 3.8 that is invalid for clouds with tops lower than about 4 km.

net effect on the energy balance at the top of the atmosphere. Those that fall below the line will produce a reduction in net radiation, or a cooling, and those above will produce warming. One can obtain the approximate cloud albedo enhancement for global average conditions by adding the clear-sky albedo, which is about 15%. As the cloud top rises, the albedo contrast between cloudy and clear conditions that will just balance the OLR change also increases. Clouds with high cold tops and low albedos can cause a significant positive change in net radiation, while low bright clouds can cause a large negative change in net radiation at the top of the atmosphere.

3.13 OBSERVATIONS OF REAL CLOUDS

The observed distribution of clouds has been estimated in two ways. Surface observers have recorded the type and fractional distribution of clouds and a long record of such observations has been compiled into a cloud climatology (Warren et al., 1986, 1988). Since about 1980, clouds have been systematically characterized from the observations of visible and infrared radiation taken from Earth orbiting satellites (Rossow and

Schiffer, 1991). Each of these data sets has its strengths and weaknesses related to the viewing geometry (up versus down) and the instrumentation (the human eye versus a radiometer). Surface observations have a much better view of cloud base, whereas satellite measurements see the tops of the highest clouds very well and provide a more direct means of estimating the visible optical depth of the clouds. Recently, radars and lidars have been flown in space that can actively scan for the vertical structure of clouds and aerosols.

Figure 3.21 shows global maps of the fractional area coverage of clouds with tops at pressures lower than 440 mb (high clouds), clouds with tops at pressures greater than 680 mb (low clouds) and clouds with tops at any pressure (total cloud amount). High clouds are concentrated in the convection zones of the tropics over equatorial South America and Africa, and a major concentration exists over Indonesia and the adjacent regions of the eastern Indian and western Pacific Oceans. Low clouds are most prevalent in the subtropical eastern ocean margins and in middle latitudes. The low cloud concentrations in the eastern subtropical oceans are associated with lower than average sea surface temperature (SST) (Fig. 7.14) and consist of stratocumulus clouds trapped below an inversion. Low clouds are heavily concentrated over the oceanic regions and are less commonly observed over land. The total cloud cover also shows a preference for oceanic regions, particularly in mid latitudes where the total cloud cover is greatest. Minima in total cloud cover occur in the subtropics in desert regions, but regions with low total cloud amounts also occur over the Caribbean Sea and over the southern subtropical zones of the Pacific, Atlantic, and Indian oceans.

Satellite measurements of the broadband energy flux also enable measurements of the spatial distribution of the cloud radiative effects whose global values are given in Table 3.2. The longwave cloud effect is the reduction of the OLR by the clouds, and so is a positive contribution to the radiation budget or warming influence on the surface climate. The largest contributions are made in the convective regions and the *intertropical convergence zone* (ITCZ) in the tropics where high clouds with cold tops are abundant (Fig. 3.22a). The reduction of absorbed solar radiation is also relatively large in these regions, since the deep convective clouds also have high albedos, but low clouds in middle latitudes are also very effective in reducing the absorbed solar radiation (Fig. 3.22b). The net effect of clouds on the energy budget at the top of the atmosphere is generally smaller than its longwave and shortwave components because in most cases they are of opposite sign. The largest net contributions are reductions in net radiation by low clouds in high latitudes and in the stratus cloud regions in the eastern subtropical oceans (Fig. 3.22c).

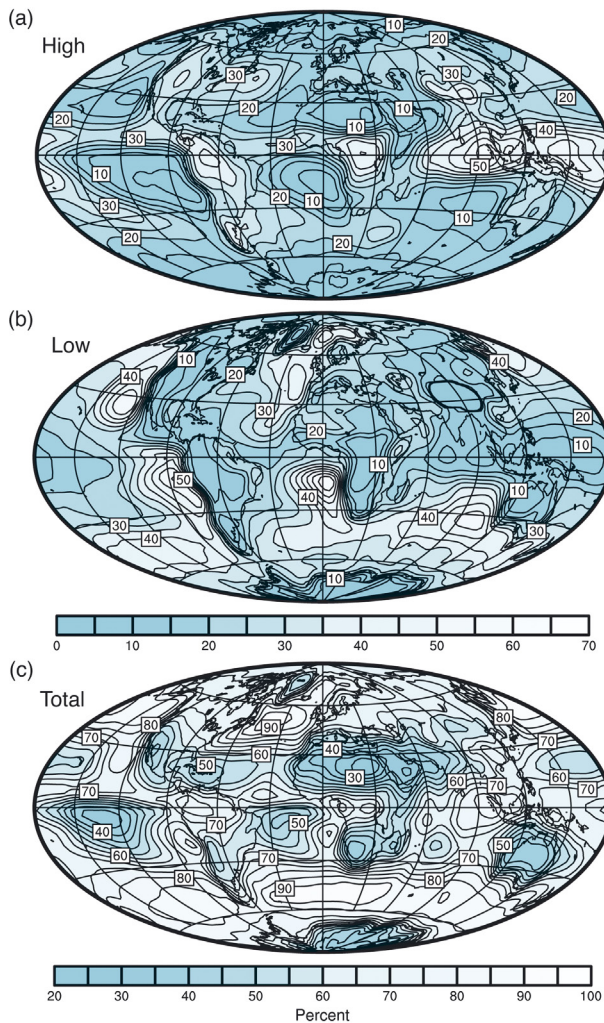


FIGURE 3.21 Annual average cloud fractional area coverage in percent estimated from satellite data under the international satellite cloud climatology project averaged for the period 1983–2009. Contour interval is 5%, lighter shade means more cloud. (a) Clouds with tops higher than 440 mb, (b) clouds with tops lower than 680 mb, and (c) all clouds. ISCCP, Rossow and Schiffer (1991).

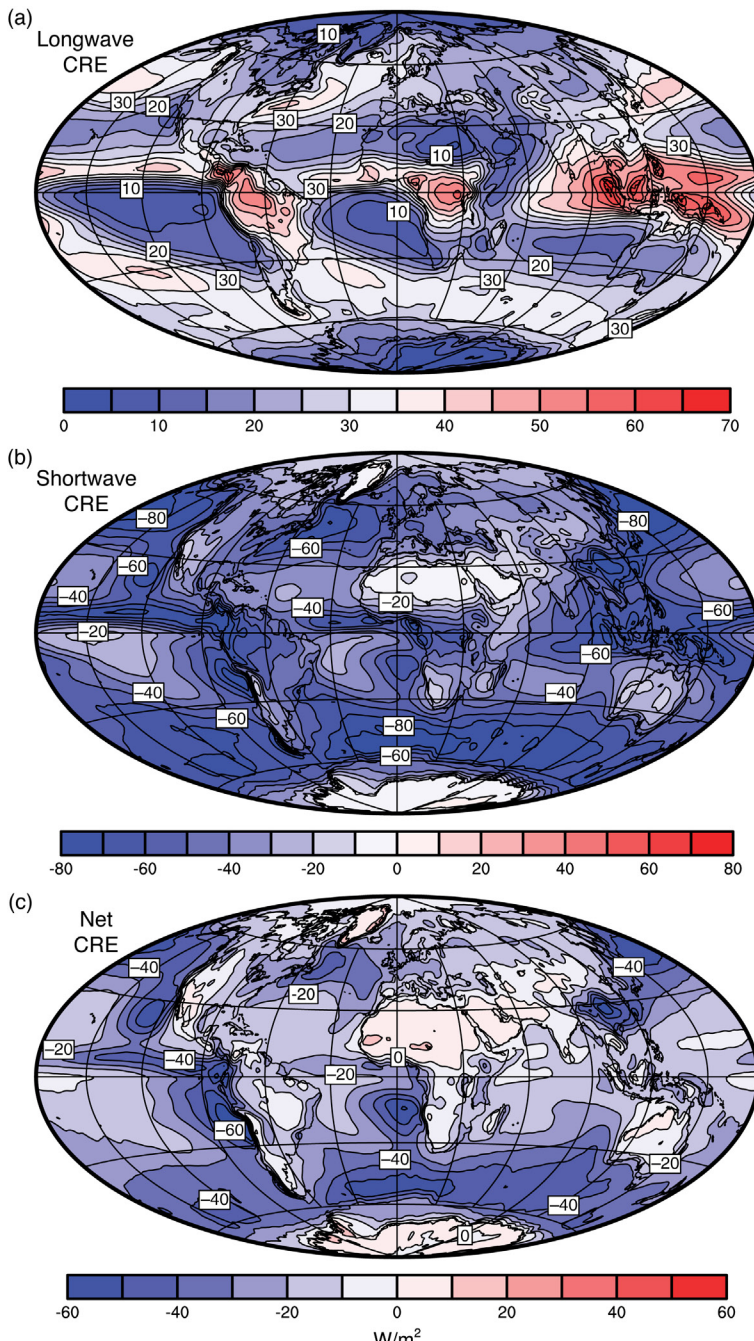


FIGURE 3.22 Annual average cloud radiative effects in W m^{-2} estimated from satellite data by the clouds and the Earth's radiant energy system (CERES) experiment. (a) Reduction of OLR caused by clouds, (b) increase in absorbed solar radiation caused by clouds (note values are negative), and (c) increase in net radiation caused by clouds. Wielicki *et al.* (1996).

EXERCISES

1. Suppose a gas that absorbs solar radiation has a uniform mixing ratio of 1 g kg^{-1} and an absorption cross-section of $5 \text{ m}^2 \text{ kg}^{-1}$. At what altitude will the maximum rate of energy absorption per unit volume occur? Assume an isothermal atmosphere with $T = 260 \text{ K}$, and a surface pressure of $1.025 \times 10^5 \text{ Pa}$, and that the Sun is directly overhead.
2. In problem 1, if the frequency range at which the absorption is taking place contains 5% of the total solar energy flux, what is the heating rate in degrees per day at the level of maximum energy absorption? What is the heating rate one scale height above and below the level of maximum energy absorption? Use the globally averaged insolation.
3. Do problem 1 with a solar zenith angle of 45° . Discuss the difference the angle makes.
4. Derive (3.23) using (3.22), (3.19) and the ideal gas law.
5. Use the model of Fig. 3.10, but distribute the solar heating such that $0.3\sigma T_e^4$ is absorbed in each of the two atmospheric layers and the remaining $0.4\sigma T_e^4$ is absorbed at the surface. Calculate the new radiative equilibrium temperature profile. How does it differ from the case where all of the solar heating is applied at the surface?
6. Place the two layers in the model of Fig. 3.10 at 2.5 and 5.0 km. Assume a fixed lapse rate of 6.5 K km^{-1} . Derive energy balance equations that include an unknown convective energy flux from the surface to the lower layer and from the lower layer to the upper layer. Solve for the temperature profile in thermal equilibrium and find the required convective energy fluxes from the surface and the lower layer. (*Hint:* Start from the top and work down.) How do the radiative and convective fluxes compare with the proportions given in Fig. 2.4?
7. For the conditions of problem 5, calculate the pure radiative equilibrium temperature profile with no convective adjustment. Plot the thermal equilibrium and pure radiative equilibrium temperature profiles from this model with the levels at 2.5 and 5.0 km and compare them with the profiles shown in Fig. 3.16. What happens to this comparison if the top level is moved up or down by 2 km? Is the dependence on the height of the layer reasonable? How do the required convective fluxes change as you move the top level up and down?
8. Suppose that tropical convective clouds give an average planetary albedo of about 0.6 compared to the cloud-free albedo of about 0.1. The insolation is about 400 Wm^{-2} , and the cloud-free OLR is about 280 Wm^{-2} . Use the simplified model of Section 3.11 to find the cloud top temperature for which the net radiative effect of these clouds will be zero. Are such temperatures observed in the tropical troposphere, and, if so, where? (Refer to Fig. 1.3.) If the surface temperature is 300 K and

the average lapse rate is 5 K km^{-1} , at what altitude would the cloud top be to make the longwave and shortwave effects of the cloud just equal and opposite?

9. For the conditions of problem 7, what is the rate of net radiative energy loss if the cloud albedos are 0.7 rather than 0.6? By how much would you need to lower the cloud tops to produce an equal reduction in net radiation?
-